Isozyme-nonselective N-Substituted Bipiperidylcarboxamide Acetyl-CoA Carboxylase Inhibitors Reduce Tissue Malonyl-CoA Concentrations, Inhibit Fatty Acid Synthesis, and Increase Fatty Acid Oxidation in Cultured Cells and in Experimental Animals*

H. James Harwood, Jr.‡, Stephen F. Petras, Lorraine D. Shelly, Lawrence M. Zaccaro, David A. Perry, Michael R. Makowski, Diane M. Hargrove, Kelly A. Martin, W. Ross Tracey, Justin G. Chapman, William P. Magee, Deepak K. Dalvie, Victor F. Soliman, William H. Martin, Christian J. Mularski, and Shane A. Eisenbeis

From the Department of Cardiovascular and Metabolic Diseases, Pfizer Global Research and Development, Groton Laboratories, Pfizer Inc., Groton, Connecticut 06340

Inhibition of acetyl-CoA carboxylase (ACC), with its resultant inhibition of fatty acid synthesis and stimulation of fatty acid oxidation, has the potential to favorably affect the multitude of cardiovascular risk factors associated with the metabolic syndrome. To achieve maximal effectiveness, an ACC inhibitor should inhibit both the lipogenic tissue isozyme (ACC1) and the oxidative tissue isozyme (ACC2). Herein, we describe the biochemical and acute physiological properties of CP-610431, an isozyme-nonselective ACC inhibitor identified through high throughput inhibition screening, and CP-640186, an analog with improved metabolic stability. CP-610431 inhibited ACC1 and ACC2 with IC_{50}s of ~50 nM. Inhibition was reversible, uncompetitive with respect to ATP, and non-competitive with respect to bicarbonate, acetyl-CoA, and citrate, indicating interaction with the enzymatic carboxyl transfer reaction. CP-610431 also inhibited fatty acid synthesis, triglyceride (TG) synthesis, TG secretion, and apolipoprotein B secretion in HepG2 cells (ACC1) with EC_{50}s of 1.6, 1.8, 3.0, and 5.7 μM, without affecting either cholesterol synthesis or apolipoprotein CIII secretion. CP-640186, also inhibited both isozymes with IC_{50}s of ~55 nM but was 2–3 times more potent than CP-610431 in inhibiting HepG2 cell fatty acid and TG synthesis. CP-640186 also stimulated fatty acid oxidation in C2C12 cells (ACC2) and in rat epitrochlearis muscle strips with EC_{50}s of 57 nM and 1.3 μM. In rats, CP-640186 lowered hepatic, soleus muscle, quadriceps muscle, and cardiac muscle malonyl-CoA with ED_{50}s of 55, 6, 15, and 8 mg/kg. Consequently, CP-640186 inhibited fatty acid synthesis in rats, CD1 mice, and ob/ob mice with ED_{50}s of 13, 11, and 4 mg/kg, and stimulated rat whole body fatty acid oxidation with an ED_{50} of ~30 mg/kg. Taken together, These observations indicate that isozyme-nonselective ACC inhibition has the potential to favorably affect risk factors associated with the metabolic syndrome.

Metabolic syndrome (also known as insulin resistance syndrome, syndrome X) is a common clinical disorder that is defined as the presence of increased insulin concentrations in association with other disorders including visceral obesity, hyperlipidemia and dyslipidemia, hyperglycemia, hypertension, and sometimes hyperuricemia and renal dysfunction (1–7). Metabolic syndrome is considered by many as a common basic defect for type 2 diabetes, android obesity, dyslipidemia, and hypertension, leading to a clustering of these diseases (1, 4, 6, 8). This syndrome has particular significance because it has been shown to be an antecedent of both type-2 diabetes and atherosclerosis, with cardiovascular events accounting for the majority of deaths in both populations (9–11). When defined using the recent guidelines of the National Cholesterol Education Program (NCEP)[1] Adult Treatment Panel III (4, 5), it is estimated that ~24% of adults in the United States alone suffer from some form of metabolic syndrome (4).

Recent studies have suggested that abnormal fatty acid metabolism may be at the core of metabolic syndrome (12–14). Acetyl-CoA carboxylase (ACC) catalyzes the rate-limiting reaction in fatty acid biosynthesis (15–17). Malonyl-CoA, the product of the ACC-catalyzed reaction, inhibits mitochondrial fatty acid oxidation through feedback inhibition of carnitine palmitoyltransferase 1 (CPT-1; Refs. 18 and 19), and therefore plays key roles both in controlling the switch between carbohydrate and fatty acid utilization in liver and skeletal muscle and also in regulating insulin sensitivity in the liver, skeletal muscle, and adipose tissue (18–20). Malonyl-CoA may also play an important regulatory role in controlling insulin secretion from the pancreas (21, 22).

Thus, in addition to inhibition of fatty acid synthesis, reduction in malonyl-CoA levels through ACC inhibition may provide a mechanism for increasing fatty acid utilization that may reduce TG-rich lipoprotein secretion (very low density lipoprotein) by the liver, alter insulin secretion by the pancreas, and improve insulin sensitivity in liver, skeletal muscle, and adipose tissue. Additionally, by increasing fatty acid utilization and by preventing increases in *de novo* fatty acid synthesis,

[1] The abbreviations used are: NCEP, National Cholesterol Education Program; ACC, acetyl-CoA carboxylase; TOFA, 5-(tetradecyloxy)-2-furancarboxylic acid, CPT-1, carnitine palmitoyltransferase-1; TG, triglyceride; ABT, aminobenzotriazole; apo, apolipoprotein; PEG, polyethylene glycol; PBS, phosphate-buffered saline; BSA, bovine serum albumin; AUC, area under the plasma concentration time curve; DMEM, Dulbecco's modified Eagle's medium; RQ, respiratory quotient.

chronic administration of an ACC inhibitor may also deplete liver and adipose tissue TG stores in obese subjects consuming a low fat diet, leading to selective loss of body fat.

Therefore, a well tolerated ACC inhibitor could effectively and simultaneously treat the multiple risk factors associated with metabolic syndrome and could have a significant impact on the prevention and treatment of the cardiovascular morbidity and mortality associated with obesity, hypertension, diabetes, and atherosclerosis.

The first reported evidence that inhibition of ACC could favorably affect the etiology of the metabolic syndrome came from studies with the long-chain fatty acid analog, 5-(tetradecyloxy)-2-furancarboxylic acid (TOFA; Refs. 23–28). In these reports, investigators demonstrated that TOFA, when converted to the CoA analog intracellularly (24), inhibited ACC activity (24), reduced fatty acid synthesis and TG secretion both in cultured hepatic cells (24, 27) and in experimental animals (23, 26, 28), reduced plasma cholesterol and TGs in experimental animals including rhesus monkeys (23, 27), and reduced body weight (25). However, the similarity of TOFA to various long-chain fatty acids called into question the specificity of the compound for ACC inhibition relative to inhibition of other long-chain fatty acyl-CoA-utilizing enzymes and therefore complicated interpretation of the findings with respect to the benefits of ACC inhibition *per se*. In addition, the existence of multiple tissue-specific ACC isoforms (15, 29–33), one primarily involved in fatty acid synthesis in the liver and adipose tissue (ACC1) and the other primarily involved in regulating fatty acid oxidation in the liver and skeletal muscle (ACC2), was not known at the time of these studies, and therefore the role of ACC1 inhibition *versus* ACC2 inhibition in the actions of TOFA was unknown.

More recently, a report by Wakil and co-workers (34) demonstrated that knock-out mice lacking ACC2 activity but maintaining a fully functional ACC1 gene locus, presented with a phenotype demonstrating a reduction in skeletal muscle malonyl-CoA concentrations, an increase in rates of muscle fatty acid oxidation, a reduced hepatic fat content, a reduction in total body fat in the face of a somewhat greater food consumption, and a reduction in plasma glucose and free fatty acid concentration relative to wild-type litter-mates, while maintaining a normal growth rate, life expectancy, and breeding capacity. These observations add further support to the concept of the utility of ACC inhibition to the treatment of metabolic syndrome. However, in these studies, it was clear that the liver and possibly also adipose tissues were compensating to some degree for the lack of ACC2-mediated control of fatty acid oxidation by increasing ACC1-mediated fatty acid synthesis (34). Indeed, in previous reports in which the efficacy of TOFA analogs was evaluated (25), investigators demonstrated the need to inhibit fatty acid production in the adipose tissue as well as in the liver, because compounds that were hepatoselective, and not peripherally available, were less effective or not effective (35). Taken together, these observations suggest that an isozyme-nonselective ACC inhibitor that would inhibit ACC2 activity in oxidative tissues such as the liver and skeletal muscle, and at the same time inhibit the activity of ACC1 in lipogenic tissues such as the liver and adipose and prevent any compensatory increases in fatty acid synthesis from attenuating the ACC2 inhibition-mediated increases in fatty acid oxidation, would have the optimal therapeutic potential for treating the multiple sequelae of metabolic syndrome.

In mid-1996, we set out to identify an ACC-specific, isozyme-nonselective ACC inhibitor for use in increasing confidence in the hypothesis that ACC inhibition-mediated reductions in fatty acid synthesis and increases in fatty acid oxidation rep-

resent a potential therapeutic approach for the treatment of the combined dyslipidemia, visceral obesity, and insulin resistance that are the hallmarks of the metabolic syndrome. In this report we describe the biochemical an physiological properties of CP-610431(Table I, inset), an isozyme-nonselective ACC inhibitor identified using a 96-well multiplexed, high throughput screening paradigm and its more metabolically stable analog CP-640186, which equally inhibit mammalian ACC1 and ACC2, reduce malonyl-CoA concentration in liver, heart, and skeletal muscle tissue, reduce fatty acid synthesis in cultured liver cells and in the liver and adipose tissue of experimental animals, increase fatty acid oxidation in cultured skeletal muscle cells and tissue slices, and reduce respiratory quotient in experimental animals. In a subsequent report,[2] we will describe the utility of CP-640186 for reducing liver, adipose, and skeletal muscle fat content, reducing whole body fat mass, and improving insulin sensitivity in chronic (up to 8-week) studies in dietarily induced rat models of the metabolic syndrome.

EXPERIMENTAL PROCEDURES

Materials—Sodium [2-^{14}C]acetate (56 mCi/mmol), [*acetyl*-^{3}H]acetyl-CoA (3.3 Ci/mmol), [1-^{14}C]palmitic acid (51 mCi/mmol), and Aquasol-2 were from PerkinElmer Life Sciences. [^{3}H]Glycerol (20 Ci/mmol) was from American Radiochemicals (St. Louis, MO). NaH[^{14}C]O$_3$ (58 mCi/mmol) was from Amersham Biosciences. Ready Safe™ liquid scintillation mixture was from Beckman Instruments (Fullerton, CA). OptiPhase "Hi-Safe" 3 liquid scintillation fluid was from Wallac-Perkin Elmer Co. (Boston, MA). Hionic-fluor liquid scintillation fluid was from Packard Instrument Co. (Meriden, CT). Dulbecco's modified Eagles' medium (DMEM), L-glutamine, and gentamicin were from Invitrogen. Heat-inactivated fetal bovine serum was from HyClone Laboratories (Logan, UT). Silica Gel 60C TLC plates were from Eastman Kodak Co. (Rochester, NY). BCA protein assay reagent was from Pierce. HepG2 cells and C2C12 cells were from the American Type Culture Collection (Rockville, MD). Mouse anti-human apoB monoclonal antibodies (MoAB-012), goat anti-human apoB polyclonal antibodies (AB-742), and human apoCIII purified standard (ALP60) were from Chemicon (Temecula, CA). Goat anti-human apoCIII polyclonal antibodies (K74140G) and biotinylated goat anti-human apoCIII polyclonal antibodies (K74170B) were from BioDesign International (Saco, ME). A streptavidin-alkaline phosphatase conjugate (RPN1234) was from Amersham Biosciences. ACC1- and ACC2-specific antibodies were purchased from Dr. Lee A. Witters, Dartmouth Medical School (Hanover, NH). Sprague-Dawley rats and CD1 mice were from Charles River (Boston, MA). C57BL/6J-ob/ob mice were from Jackson Laboratory (Bar Harbor, ME). RMH 3200 laboratory meal was from Agway Inc. (Syracuse, NY). AIN76A semi-purified rodent diet was from Research Diets Inc. (New Brunswick, NJ). All other chemicals and reagents were from previously listed sources (36, 37).

Preparation of ACC1 from Liver and Adipose Tissue and ACC2 from Skeletal and Cardiac Muscle—ACC1 was prepared from rat liver or rat adipose tissue, and ACC2 was prepared from rat skeletal or cardiac muscle tissue essentially as previously described (38) with the following modifications. Male Sprague-Dawley rats weighing 150–200 g were fasted for 2 days and then fed a high sucrose diet (AIN76A) for 3 days (induces ACC1 activity ~10-fold), at which time they were killed by CO$_2$ asphyxiation. The livers (for ACC1 preparation), epididymal adipose tissue (for ACC1 preparation), skeletal muscle tissue (for ACC2 preparation), and cardiac muscle tissue (for ACC2 preparation) were removed, rinsed in ice-cold PBS, and homogenized in 5 volumes of homogenization buffer (50 mM potassium phosphate (pH 7.5) 10 mM EDTA, 10 mM 2-mercaptoethanol, 2 mM benzamidine, 0.2 mM PMSF, 5 mg/liter each leupeptin, aprotinin, and antitrypsin) in a Waring blender for 1 min at 4 °C. Adipose tissue was frozen in liquid N$_2$ and then pulverized in liquid N$_2$ prior to homogenization as described above. All subsequent operations were carried out at 4 °C. The homogenate was made 3% with respect to polyethylene glycol (PEG) by the addition of 50% PEG solution and centrifuged at 20,000 × g for 15 min. The resulting supernatant was adjusted to 5% PEG with the addition of 50% PEG solution and stirred for 5 min. The pellet (contains ACC activity) was collected by centrifugation at 20,000 × g for 20 min, rinsed with 4 °C double-

---

[2] H. J. Harwood, S. F. Petras, L. D. Shelly, V. F. Soliman, and D. A. Perry, manuscript in preparation.

distilled H_2O to remove excess PEG, and resuspended in one-fourth the original homogenate volume with homogenization buffer. Ammonium sulfate (200 g/liter) was slowly added with stirring. After 45 min the enzyme was collected by centrifugation for 30 min at $20,000 \times g$, resuspended in 10 ml of 50 mM HEPES (pH 7.5) buffer containing 0.1 mM DTT, 1.0 mM EDTA, and 10% glycerol, and desalted on a G-25 column (2.5 cm $\times$ 50 cm) equilibrated with the same buffer. The desalted enzyme preparation was stored in aliquots at -70 °C. When isolated under these conditions, partially purified rat adipose tissue ACC was exclusively ACC1, partially purified rat heart ACC was exclusively ACC2, partially purified rat skeletal muscle ACC was exclusively ACC2, and partially purified rat liver ACC was a mixture of both ACC1 and ACC2 in a 85:15 ratio, as demonstrated by immunoblotting with specific polyclonal antibodies after PAGE. Immediately prior to use, frozen aliquots of the above fractions were thawed, diluted to 500 μg/ml in buffer containing 50 mM HEPES (pH 7.5), 10 mM $MgCl_2$, 10 mM tripotassium citrate, 2.0 mM DTT, and 0.75 mg/ml fatty acid-free BSA and the ACC was citrate-activated by preincubation at 37 °C for 30 min.

Measurement of Acetyl-CoA Carboxylase Inhibitory Activity—The procedure for measuring ACC1 and ACC2 activity utilizes a radiochemical method (38) that measures incorporation of [^{14}C]bicarbonate into [^{14}C]malonyl-CoA and separates product from unused substrate at the end of the reaction through acidification, which serves to both quench the reaction and remove residual radiolabeled substrate as $^{14}CO_2$. For measurement of ACC activity and assessment of ACC inhibition, test compounds were dissolved in Me_2SO and 1.0 μl was placed in 0.5-ml polypropylene tubes. Control tubes contained 1.0 μl of Me_2SO alone. All assay tubes received 139 μl of substrate buffer containing 50 mM HEPES (pH 7.5), 2.0 mM $MgCl_2$, 2.0 mM tripotassium citrate, 2 mM DTT, 0.75 mg/ml BSA, 25 μM acetyl-CoA, 4.0 mM ATP, and 12.5 mM $KH[^{14}C]O_3$ (2×10^6 cpm). The reaction was initiated by the addition of 10 μl of citrate-activated ACC solution. After 7 min the reaction was stopped by the addition of 50 μl of 6 N HCl and 150 μl of the quenched reaction mixture was transferred to glass scintillation vials and evaporated to dryness at 90 °C for 1 h. The dried vials were cooled, 0.5 ml of water and 5.5 ml of Beckman Readisafe liquid scintillation fluid were added, and the radioactivity was determined in a Beckman LS6500 liquid scintillation counter. Tubes that received HCl before citrate-activated ACC solution served as blanks. ACC activity is expressed as nanomoles of $KH[^{14}C]O_3$ incorporated into malonyl-CoA per min of incubation at 37 °C per mg of protein.

ACC Inhibition High Throughput Screening Format—The method for measuring ACC activity and inhibition was adapted to high throughput (80 plate-per-assay scale) inhibitor screening format as follows: compounds dissolved in Me_2SO in 96-well multiplexed format were added to wells of a 96-well plate containing 90 μl of assay buffer consisting of 50 mM HEPES (pH 7.5), 2.0 mM $MgCl_2$, 2.0 mM tripotassium citrate, 2 mM DTT, 0.75 mg/ml BSA, 25 μM acetyl-CoA, and 4.0 mM ATP (final compound concentration 5.0 μM). Plates were then transferred to a fume hood and were supplied with 10 μl of a solution containing 12.5 mM $NaH[^{14}C]O_3$ (2×10^6 cpm). Reactions were then initiated by addition of 10 μl of partially purified, citrate-activated rat liver ACC solution (5 μg of protein) isolated from fasted, high sucrose diet-refed rats (85% ACC1, 15% ACC2) and incubated for 10 min at room temperature. After incubation, reactions were terminated by addition of 10 μl of 6 M HCl and plates were permitted to stand in the hood for 2 h to allow $^{14}CO_2$ liberation. Plates were then transferred to a 65 °C vacuum oven fitted with an elaborate system of NaOH traps and charcoal filters between the vacuum oven and house vacuum system to prevent both contamination by residual $^{14}CO_2$ and corrosion by the evaporated HCl. Monitoring the entrapment of $^{14}CO_2$ and HCl between the vacuum oven and house line revealed that all $^{14}CO_2$ was trapped in the first of the NaOH traps and little or none reached the charcoal filter for final entrapment. The HCl was likewise trapped by the first several NaOH traps, and they were replaced routinely as their pH was reduced. Plates remained in the vacuum oven overnight. The next morning, residue in the dried wells (contains [^{14}C]malonyl-CoA) was resuspended in 30 μl of water, dissolved in 145 μl of OptiPhase "Hi-Safe" 3 liquid scintillation fluid with vigorous shaking, sealed, and transferred to pre-programmed robotics for radioactivity assessment. By selecting for inhibitors that inhibited hepatic ACC activity by 75%, we selected for compounds that inhibited ACC1 activity. We then selected for those that also equally inhibited ACC2 in secondary specificity assays.

Measurement of HepG2 Cell Cholesterol and Fatty Acid Synthesis—Cholesterol and fatty acid synthesis were evaluated in HepG2 cells by measuring incorporation of [2-^{14}C]acetate into cellular lipids as previously described (36, 37) with the following modifications to allow simultaneous assessment of both cholesterol and fatty acid synthesis. After

collection and assessment of the hexane fraction containing cholesterol and nonsaponifiable lipids as previously described (36, 37), the remaining aqueous phase (containing fatty acid sodium salts) was acidified to pH $<$ 2 by addition of 0.5 ml of 12 M HCl. The resulting mixtures were then transferred to glass conical tubes and extracted three times with 4.5 ml of hexane. The pooled organic fractions were dried under nitrogen, resuspended in 50 μl of chloroform:methanol (1:1, v/v), and applied to 1×20-cm channels of Silica Gel 60C TLC plates. Channels containing non-radioactive fatty acids were included on selected TLC plates as separation markers. TLC plates were developed in hexane:diethyl ether:acetic acid (70:30:2) and air-dried, and the region of chromatograms corresponding to fatty acid mobility were removed and assessed for radioactivity in Aquasol-2 using a Beckman LS6500 liquid scintillation counter. Cholesterol and fatty acid synthesis are expressed as dpm [2-^{14}C]acetate/mg of cellular protein incorporated into either cholesterol or saponifiable lipids during the 6-h incubation at 37 °C.

Measurement of HepG2 Cell TG Synthesis and Secretion—HepG2 cells grown in T-75 flasks as previously described (36, 37) were seeded into 24-well plates at $4-6 \times 10^5$ cells/well and maintained in a humidified, 5% CO_2 atmosphere at 37 °C for 48 h. Media were then removed and replaced with fresh media containing 0.2% $Me_2SO \pm$ test compound. One hour after compound addition, 25 μl of media containing 50 μCi of [^{3}H]glycerol was added to each incubation well. Plates were then sealed with parafilm to avoid evaporation, and cells were incubated at 37 °C for 6 h with gentle shaking. After incubation, the media was removed and the cells were washed three times with PBS and scraped from wells into PBS. Lipids were extracted from the media and the cell lysate with chloroform-methanol (2:1) and applied to 1×20-cm channels of Silica Gel 60C TLC plates. Channels containing non-radioactive TGs were included on selected TLC plates as separation markers. TLC plates were developed in petroleum ether:diethyl ether:acetic acid (75:25:1), air-dried, and the region of chromatograms corresponding to TG mobility were removed and assessed for radioactivity in Aquasol-2 using a Beckman LS6500 liquid scintillation counter. TG synthesis and TG secretion are expressed as dpm [^{3}H]glycerol/mg of cellular protein incorporated into cellular TGs or secreted into the culture medium during the 6-h incubation at 37 °C.

Measurement of HepG2 Cell ApoB and ApoCIII Secretion—HepG2 cells were grown in DMEM containing 10% fetal bovine serum in 96-well plates in a humidified, 5% CO_2 atmosphere at 37 °C until they are ~70% confluent. On the day of experimentation, media were removed from each well and replaced with fresh media containing 0.2% $Me_2SO \pm$ test compound. Twenty-four hours later, growth medium was collected and assessed for apoB content as previously described (39, 40). Growth medium was also assessed for apoCIII content essentially as described for assessing apoB content, except that BioDesign K74140G affinity-purified polyclonal goat anti-human apoCIII antibody solution (5.0 mg/ml in PBS) was used as the capture antibody, BioDesign K74170B biotinylated, affinity-purified polyclonal goat anti-human apoCIII antibody (1:16,000 dilution in PBS containing 1% BSA and 0.05% Tween 20) was used as the secondary antibody, and Amersham RPN1234 streptavidin-alkaline phosphatase (1:600 dilution in PBS containing 1% BSA and 2 mM $MgCl_2$) was used as the detection enzyme conjugate. ApoCIII concentrations were calculated from a standard curve for purified apoCIII standards (0.01–20 ng) run in parallel.

Measurement of C2C12 Cell and Epitrochlearis Muscle Fatty Acid Oxidation—C3H mouse myoblast (C2C12) cells were grown in DMEM containing 10% fetal bovine serum in 96-well plates in a humidified, 5% CO_2 atmosphere at 37 °C until they were no more than 70% confluent. On the day of study, the medium was removed, cells were washed with 0.25% trypsin plus 0.03% EDTA solution, then incubated in 2.0 ml of trypsin-EDTA solution without shaking for ~5 min to allow cells to detach from the flask. Trypsin-released cells were resuspended with 6–8 ml of pH 7.4 assay buffer (20 mM HEPES, 25 mM $NaHCO_3$, 1.2 mM KH_2PO_4, 3 mM glucose, 114 mM NaCl, 4.7 mM KCl, 1.2 mM $MgSO_4$, 2.5 mM $CaCl_2$, 1% ultra fatty acid-free BSA) to a cell density of 1.5 million cells/ml. Cell suspension aliquots of 2.0 ml were added to 25-ml Erlenmeyer flasks and incubated for 30 min at 37 °C in a shaking water bath. Epitrochlearis muscle was removed from male 8-week-old Sprague-Dawley rats after cervical dislocation and placed into 4.5 ml of pH 7.4 assay buffer (see above) in a 25-ml Erlenmeyer flask. Muscle strips were then pre-incubated for 30 min at 37 °C in a shaking water bath. After pre-incubation, 0.5-ml aliquots of assay buffer containing various concentrations of test compound were added to each flask and were followed immediately by 80 μl (C2C12 cells) or 160 μl (muscle strips) of a solution containing 12% ultra fatty acid-free BSA and 12.7 mM [1-^{14}C]palmitate (3.4 μCi; 1.0 μCi/μmol). Flasks were then filled with a 5% CO_2 atmosphere, capped with a rubber stopper into which a center

well was inserted, and incubated for 2 h at 37 °C in a shaking water bath. After incubation, the reaction was terminated by addition of 0.5 ml of a 60% perchloric acid solution, a 300-μl volume of benzethonium hydroxide was added to each center well, and flasks were incubated overnight at room temperature to allow for quantitative capture of the released $^{14}CO_2$. After incubation, stoppers were removed from the flasks, the center well cups were cut into 7-ml scintillation vials containing 6.0 ml of Hionic-fluor liquid scintillation fluid, and the radioactivity assessed in a Beckman LS6500 liquid scintillation counter. Rates of fatty acid oxidation are expressed as nanomoles of $^{14}CO_2$ released/ min of incubation per 10^6 cells or per mg of tissue.

Studies Using Experimental Animals—All procedures using experimental animals were approved by the Institutional Animal Care and Use Procedures Review Board. Sprague-Dawley rats, C57BL/6J-ob/ob mice, or CD1 mice, were given food (RMH3200 or AIN76A) and water *ad libitum* and treated orally at a volume of 1.0 ml/200 g of body weight (rats) or 0.25 ml/25 g of body weight (mice) with either an aqueous solution containing 0.5% methyl cellulose (vehicle) or an aqueous solution containing 0.5% methyl cellulose plus test compounds.

Measurement of Hepatic Fatty Acid Synthesis—Hepatic incorporation of [2-^{14}C]acetate into TGs was essentially as previously described for assessment of hepatic sterol synthesis (36, 41) with the following modifications to allow for assessment of fatty acid synthesis. Briefly, animals given food and water *ad libitum* were treated orally at a volume of 1.0 ml/200 g of body weight (rat) or at a volume of 0.25 ml/25 g of body weight (mice) with either an aqueous solution containing 0.5% methyl cellulose (vehicle) or an aqueous solution containing 0.5% methyl cellulose plus test compound. One to 4 h after compound administration, animals received an intraperitoneal injection of 0.5 ml (rat) or 0.2 ml (mouse) of [2-^{14}C]acetate (64 μCi/ml; 56 mCi/mmol). One hour after radiolabel administration, animals were killed by CO_2 asphyxiation and two 0.75-g liver pieces were removed and saponified at 70 °C for 120 min in 1.5 ml of 2.5 M NaOH. After saponification, 2.5 ml of absolute EtOH were added to each sample and the solutions were mixed and allowed to stand overnight. Petroleum ether (4.8 ml) was then added to each sample, and the mixtures were first shaken vigorously for 2 min and then centrifuged at $1000 \times g$ in a benchtop Sorvall for 5 min. The resultant petroleum ether layers, which contain nonsaponifiable lipids, were removed and discarded. The remaining aqueous layer was acidified to pH < 2 by addition of 0.6 ml of 12 M HCl and extracted two times with 4.8 ml of petroleum ether. The pooled organic fractions were transferred to liquid scintillation vials, dried under nitrogen, dissolved in 7 ml of Aquasol liquid scintillation fluid, and assessed for radioactivity using a Beckman 6500 liquid scintillation counter. Inhibition of fatty acid synthesis is expressed as the concentration required to reduce by 50% the [2-^{14}C]acetate incorporated into saponifiable lipids during the interval between [2-^{14}C]acetate injection and CO_2 asphyxiation.

Measurement of Tissue Malonyl-CoA Concentration—Direct assessment of malonyl-CoA production in tissues that either do (*e.g.* liver and adipose tissue) or do not synthesize fatty acids (*e.g.* skeletal muscle), through its stoichiometric conversion to radiolabeled palmitate in the presence of purified fatty acid synthetase and radiolabeled acetyl-CoA, can also be used to determine ACC inhibition in those tissues as previously described by McGarry *et al.* (42). Briefly, Sprague-Dawley rats given food and water *ad libitum* were treated orally at a volume of 0.5 ml/200 g of body weight with either an aqueous solution containing 0.5% methyl cellulose (vehicle) or an aqueous solution containing 0.5% methyl cellulose plus test compound. One hour after compound administration, rats were anesthetized with pentobarbital and tissue samples were removed, immediately freeze-clamped, placed in a cryotube, and immersed in liquid N_2 in the following order to minimize blood-flow interruption during harvesting: complete soleus muscle from both legs (combined weight: 0.2–0.3 g), 2.0 g of gastrocnemius muscle, 2.0 g of quadriceps muscle, 2.0 g of adipose tissue, 2.0 g of liver, and the entire heart (0.5–1.0 g). Frozen tissues were first pulverized under liquid nitrogen, and then 1.0 g of the powdered tissues were extracted with 4 ml of 10% (w/v) $HClO_4$, neutralized to pH 6.0 with 5 M KOH, and centrifuged at 3500 rpm for 10 min in a Sorval RT6000 benchtop centrifuge to remove particulate residue. For the soleus muscle, the entire tissue was homogenized in 1.2 ml of $HClO_4$ and then neutralized and clarified as described above. Measurements of malonyl-CoA concentration in tissue extracts were carried out in duplicate in 15-ml polypropylene screw-capped tubes. Reaction mixtures, in a final volume of 1.025 ml of 250 mM potassium phosphate buffer (pH 7.0), containing 2.5 mM dithiothreitol, 2.0 mM EDTA, 0.2 mM NADPH, 1 mg/ml fatty acid-free bovine serum albumin, 0.68 μM [^{3}H]acetyl-CoA (~150,000 dpm/nmol), 2.0 nM malonyl-CoA standard, and either 100 μl of liver extract or 200 μl of skeletal muscle, heart, or adipose tissue extract,

were mixed with a 10-μl aliquot containing 25 milliunits of purified (as previously described (Ref. 42)) fatty acid synthetase (5 μg of protein) and were incubated at 37 °C for 45 min. After incubation, reactions were terminated by addition of 25 μl of 70% (w/v) $HClO_4$ and nascent palmitate was extracted by addition to each tube of 1 ml of absolute EtOH and then 5 ml of petroleum ether. After vigorous mixing for 30 s and centrifugation at 2000 rpm for 5 min in a Sorval RT6000 benchtop centrifuge to facilitate phase separation, 4.0 ml of the petroleum ether phase was transferred to a second tube containing 2 ml of water, shaken, recentrifuged, and 2.5 ml of the petroleum ether phase was transferred to liquid scintillation vials, dried, and assessed for radioactivity in a liquid scintillation counter after addition of 6 ml of Aquasol liquid scintillation fluid. Blanks containing no added malonyl-CoA or tissue extract are included with each series of determinations and subtracted from all values. Malonyl-CoA concentration per gram of tissue was calculated using the ratio of one molecule of [^{3}H]acetyl-CoA incorporated into palmitate for each seven molecules of malonyl-CoA present in the tissue extract. Inhibition of malonyl-CoA production is expressed as the concentration required to reduce by 50% the dpm [^{3}H]acetyl-CoA incorporated into palmitate during the 45-min incubation at 37 °C.

Measurement of Respiratory Quotient—Acute modulation of whole-body fatty acid utilization was assessed by measuring changes in the respiratory quotient (RQ, the ratio of CO_2 production to O_2 consumption; Ref. 43) using an open circuit, indirect calorimeter (Oxymax, Columbus Instruments, Columbus, OH). Briefly, male Sprague-Dawley rats (350–400 g) housed under standard laboratory conditions, either fed chow, fasted, or fasted and refed a diet high in sucrose for 2 days prior to experimentation were removed from their home cages, weighed, and placed in sealed chambers ($43 \times 43 \times 10$ cm) of the calorimeter (one rat per chamber). The chambers were placed in activity monitors. The calorimeter was calibrated before each use, air flow rate was adjusted to 1.6 liters/min, and the system settling and sampling times were set to 60 and 15 s, respectively. Base-line oxygen consumption, CO_2 production, and ambulatory activity were measured every 10 min for up to 3 h before treatment. After collecting base-line data, the chambers were opened and rats were given a 1.0-ml oral bolus of either an aqueous 0.5% methylcellulose solution (vehicle control) or an aqueous 0.5% methylcellulose solution containing test compound and then returned to the Oxymax chambers. Measurements were made every 10 min for an additional 3–6 h after dose. Fed vehicle controls were used to assess effects produced by vehicle administration and by drift in the RQ measurement during the course of the experimentation (if any). Overnight-fasted, vehicle-treated controls were used to determine maximal potential RQ reduction. For comparison purposes one group of rats received a selective β3-adrenergic receptor agonist (CL-316243; 1 mg/ kg). Changes in RQ in response to compound administration were calculated by dividing the average of the post-dosing RQ values (excluding values obtained during time periods where ambulatory activity exceeds 100 counts) by the average of the pre-dosing base-line values (excluding the first five values and values obtained during time periods where ambulatory activity exceeds 100 counts) and were expressed as percentage change from base line.

Measurement of Plasma and Tissue Drug Levels—To 100-μl aliquots of plasma were added 10 μl of an internal standard (2.5 μg/ml CP-633196 in methanol), 1 ml of water, and 3 ml of methylene chloride. After vigorous mixing and centrifugation, the organic layers were removed, evaporated to dryness under N_2, and the residue was reconstituted with 100 μl of mobile phase (50% methanol, 50% 10 mM ammonium acetate, pH 6). Liver tissue (1.0 g) was homogenized in 3 ml of water, and 100 μl of the homogenate was extracted as above except that a larger volume of methylene chloride (5 ml) was used. Skeletal muscle tissue (1.0 g) was homogenized in a mixture of 3 ml of 10% trichloroacetic acid and 3 ml of methanol, and 175 μl of the homogenate was extracted with 5 ml of methylene chloride as outlined above for liver. For determination of half-life in hepatic microsomes, 100-μl aliquots of liver microsome incubates were removed at various time intervals and extracted as outlined above. Aliquots (20–40 μl) of reconstituted samples were injected onto a Monitor column (5-μm, C18; 150×4.6 mm, inner diameter; Columns Engineering). Separation was achieved using an isocratic gradient with 85% methanol and 15% 10 mM ammonium acetate (pH 6) with a flow rate of 0.5 ml/min. Quantitation of CP-640186 and internal standard was done using a PerkinElmer Sciex API3000 (Applied Biosystems, Toronto, Canada) mass spectrometer. Detection was done using multiple reaction monitoring with turbo ion spray source in the negative ionization mode. The ion transitions were monitored at m/z 486.2 (M − H) to m/z 205 (product ion), and m/z 472.0 (M − H) to m/z 205 (product ion) for CP-640,186 and CP633,196, respectively.

FIG. 1. **Inhibition of ACC1 and ACC2 activity by CP-610431.** Aliquots of rat liver ammonium sulfate fraction (90% ACC1, 10% ACC2), rat adipose ammonium sulfate fraction (100% ACC1), rat skeletal muscle ammonium sulfate fraction (100% ACC2), and rat heart ammonium sulfate fraction (100% ACC2) containing 5.0 μg of protein were incubated with ACC substrates and cofactors, and concentrations of CP-497485 ranging between 1.0 nM and 30 μM for 10 min at 37 °C as outlined under "Experimental Procedures." After incubation, unreacted $NaH[^{14}C]O_3$ was removed by acidification, the reaction mixture was dried, and the dried residue, containing nascent [^{14}C]malonyl-CoA, was resuspended in Redisafe liquid scintillation fluid and assessed for radioactivity as outlined under "Experimental Procedures." Shown is the percentage of control ACC activity, presented as the mean of triplicate determinations, as a function of CP-497485 concentration. Control ACC specific activity was as follows: liver, 54.5 nmol/min/mg; heart, 4.37 nmol/min/mg, skeletal muscle, 6.59 nmol/min/mg; adipose tissue, 4.42 nmol/min/mg.
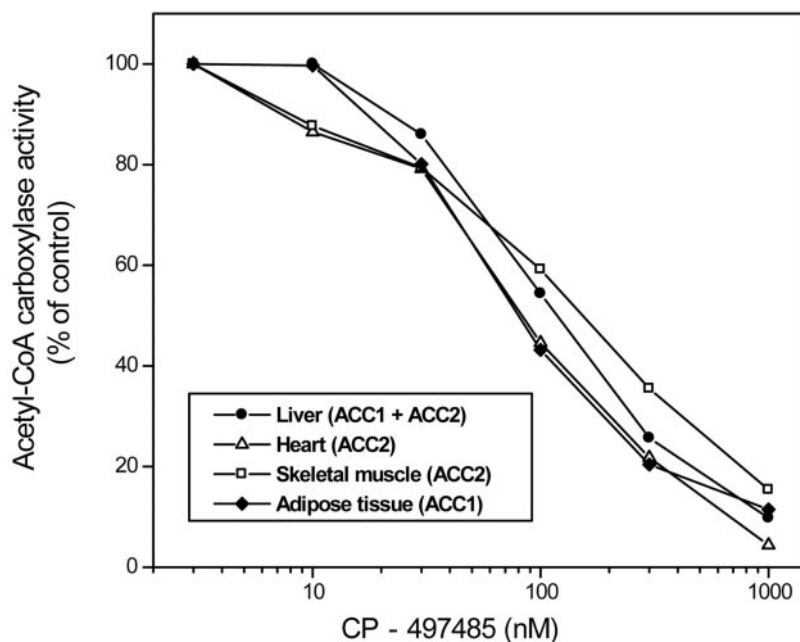
The linear dynamic range was between 5 ng/ml (lower limit of quantification) and 1 μg/ml (upper limit of quantification).

Measurement of Rat Pharmacokinetic Parameters—Four male Sprague-Dawley rats (~250 g), surgically prepared with jugular vein catheters, received a 5 mg/kg intravenous dose of CP-640186 in PEG 400 solution and four animals received a 10 mg/kg oral dose of CP-640186 in 0.5% methylcellulose. Blood samples (200 μl) were collected from the indwelling jugular vein catheter up to 24 h after dose administration and placed into heparinized tubes. Samples were centrifuged at 3000 rpm for 10 min and the plasma removed and stored frozen before analysis. Pharmacokinetics parameters were estimated using WinNonlin (version 1.3). Terminal elimination rate constant (K_{el}) was determined by linear regression of the log plasma concentrations. The terminal elimination half-life ($t_{1/2}$) was calculated from 0.693/K_{el}. The area under the plasma concentration time curve (AUC) was calculated to the last time point at which drug could be measured using the linear trapezoidal rule and extrapolated to infinity by using K_{el}. Clearance was calculated by the relationship dose/AUC. The volume of distribution was calculated by the relationship clearance/K_{el}. Oral bioavailability was calculated from the ratio of AUCs after oral and intravenous doses after normalizing for the dose.

RESULTS

Identification of CP-497485 Using a 96-well Multiplex High Throughput Screening Paradigm—To identify isozyme-nonselective ACC inhibitors, we adapted to 96-well plate format a method that measures incorporation of [^{14}C]bicarbonate into [^{14}C]malonyl-CoA and separates product from unreacted substrate by acidification and removal of residual radiolabeled substrate as $^{14}CO_2$. This method possesses the advantages of sensitivity, ease of separation of product from unreacted substrate, applicability to use of partially pure enzyme preparations, and direct product measurement that facilitated the high throughput inhibition screening effort.

Our search for ACC inhibitors focused on those that either antagonize citrate-mediated ACC activation or inhibit enzymatic activity by mimicking acetyl-CoA or acyl-CoA molecules. Therefore, concentrations of citrate and acetyl-CoA were employed that yielded half-maximal activation (2 mM citrate; K_a = 2.7 mM) and half-maximal activity (30 μM acetyl-CoA; K_m = 33 μM), respectively, whereas saturating concentrations of ATP (4 mM; K_m = 43 μM) and KHCO$_3$ (12.5 mM; K_m = 2.5 mM) were employed. Additionally, by using partially purified ACC isolated from the livers of rats that had been fasted and then refed a high carbohydrate diet (induces ACC1 activity ~10-fold;

isozyme distribution: 85% ACC1, 15% ACC2), and by identifying compounds that inhibited ACC activity by greater than 75%, we selected for compounds that inhibited ACC1 activity. Inhibition of ACC2 activity was then determined in secondary specificity assays. Under these assay conditions, the IC$_{50}$ values of known inhibitors of ACC activity, stearoyl-CoA, palmitoyl-CoA, and myristoyl-CoA were 0.6, 1.5, and 23 μM, respectively, similar to that reported in the literature (44).

The activity of hits identified using this format were confirmed, and subsequent potency evaluations yielded a number of actives that were considered worthy of further pursuit. Substructure searches around core structures and subsequent inhibitory activity evaluation confirmed that all were *bona fide* active series. The most attractive of these series is exemplified by the prototype CP-497485, a racemic compound that exhibited an IC$_{50}$ against the partially purified rat liver enzyme of 250 nM.
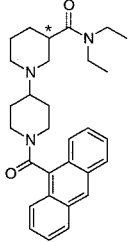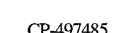
Inhibition of ACC1 and ACC2 by CP-497485 and Its R-Enantiomer, CP-610431—In mammals, ACC exists as two tissue-specific isozymes, a 265-kDa isozyme (ACC1) present in lipogenic tissues such as liver and adipose tissue and a second 280-kDa isozyme (ACC2) present in oxidative tissues such as liver, skeletal muscle, and cardiac muscle (15, 29–33). Using antibodies specific for ACC1 and ACC2, exclusivity of ACC1 in rat adipose tissue, ACC2 in rat heart, ACC2 in rat skeletal muscle, and the presence of both isozymes in an 85:15 ratio in fasted, high sucrose diet-refed rat liver was demonstrated by immunoblotting after PAGE. As shown in Fig. 1, CP-497485 inhibited ACC activity partially purified from liver, heart, skeletal muscle, and adipose tissue with IC$_{50}$ values of 120, 90, 150, and 80 nM, respectively, indicating a lack of isozyme specificity for the compound.

Resolution of CP-497485 into its two enantiomers revealed that the *R*-enantiomer, CP-610431, was considerably more potent than the racemate in inhibiting rat ACC1 (IC$_{50}$ = 35.7 ± 9.3 (S.D.) ± 1.9 (S.E.); n = 16) nM) and ACC2 (IC$_{50}$ = 55 nM), whereas the *S*-enantiomer, CP-610432, did not substantially inhibit either ACC isoform at concentrations of up to 3 μM (chiral separation enantiomer efficacy data shown in Table I).

CP-610431 also inhibited mouse and cynomolgus macaque ACC1 and ACC2 activities. As noted above for the rat, mouse

TABLE I

Inhibition of ACC activity by CP-497485 and its enantiomers
CP-610431 and CP-610432

Aliquots of rat liver ammonium sulfate fraction (90% ACC1, 10% ACC2) and rat skeletal muscle ammonium sulfate fraction (100% ACC2) containing 5.0 μg protein, prepared as described under "Experimental Procedures," were incubated with ACC substrates and cofactors, and concentrations of either CP-497485, CP-610431, or CP-610432 ranging between 1.0 nM and 30 μM for 10 min at 37 °C as outlined under "Experimental Procedures." After incubation, unreacted NaH[^{14}C]O$_3$ was removed by acidification, the reaction mixture was dried, and the dried residue, containing nascent [^{14}C]malony1-CoA, was resuspended in Redisafe liquid scintillation fluid and assessed for radioactivity as outlined under "Experimental Procedures." Inhibition of ACC activity is expressed as the concentration of inhibitor required to prevent by 50% the incorporation of NaH[^{14}C]O$_3$ into malonyl-CoA during the 10-min incubation.

| | | Inhibition of ACC activity (IC$_{50}$; nM) | |
	Configuration at asterisk	Rat liver isozyme (ACC1)	Rat skeletal muscle isozyme (ACC2)
CP-497485	R/S	265	460
CP-610431	R	107	112
CP-610432	S	> 1,000	> 1,000

and cynomolgus macaque liver also contained both ACC1 and ACC2, whereas mouse and cynomolgus macaque skeletal muscle contained only ACC2. Likewise, when mice and cynomolgus macaques were fasted and then re-fed a high sucrose diet for 2 days, the hepatic ACC1 to ACC2 ratio was ~6. Under these isolation conditions, rat, mouse, and cynomolgus macaque liver ACC activity averaged 29, 31.3, and 2.5 nmol/min/mg, whereas their skeletal muscle ACC averaged 3.4, 3.5, and 0.8 nmol/min/ mg, respectively. CP-610431 inhibited both liver and skeletal muscle ACC activity from all three species with essentially equal potency (rat, 36 *versus* 55 nM; mouse, 50 *versus* 63 nM; cynomolgus macaque, 70 *versus* 26 nM), further demonstrating the isozyme nonselectivity and pan-species efficacy of ACC inhibition by CP-610431.

CP-497485 and CP-610431 both showed a high degree of specificity for ACC inhibition relative to inhibition of pyruvate carboxylase or propionyl-CoA carboxylase, exhibiting no inhibitory activity toward either of these enzymes at concentrations of up to 100 μM. CP-497485 and CP-610431 also both showed a high degree of specificity for inhibition of mammalian ACC *versus* fungal ACC. For example, CP-497485 (IC$_{50}$ = 250 nM *versus* rat ACC1) showed no inhibition of *Candida albicans* ACC at concentrations of up to 10 μM and CP-610431 (IC$_{50}$ = 36 nM *versus* rat ACC1) only modestly inhibited the *C. albicans* (IC$_{50}$ = 6.0 μM) and *Aspergillus fumigatus* (IC$_{50}$ = 1.1 μM) enzymes. Consistent with the enantiomer-specific inhibition of mammalian ACC, the less active enantiomer, CP-610432, was also less active *versus* the fungal enzyme, demonstrating no inhibition of the *C. albicans* enzyme at concentrations of up to 100 μM and only weakly inhibiting the *A. fumigatus* enzyme with an IC$_{50}$ of 62 μM.

Kinetics of ACC Inhibition by CP-610431—ACC-catalyzed carboxylation of acetyl-CoA to form malonyl-CoA proceeds via a two-step process, a biotin carboxylase reaction and a carboxyl transferase reaction (38, 45, 46). Fatty acyl-CoAs inhibit ACC

activity by competing with acetyl-CoA for binding within the active center (47). Citrate allosterically activates ACC by competing with this fatty acyl-CoA mediated enzyme inhibition (48). Detailed kinetic analyses of the catalytic mechanism of action of the ACC enzyme previously reported in the literature (45, 46) have suggested that the substrates bicarbonate and acetyl-CoA and the allosteric effectors citrate and fatty acyl-CoA all bind to overlapping regions within an area of the active center that catalyzes the enzymatic second half-reaction, that of the carboxyl transfer reaction, and that this site is distinct from the ATP binding site involved in CO$_2$ fixation in the enzymatic first half-reaction.

As shown in Fig. 2, CP-610431 inhibits ACC noncompetitively with respect to acetyl-CoA, bicarbonate, and citrate but uncompetitively with respect to ATP. The reaction is reversible, as demonstrated by the absence of time-dependent loss of enzyme activity upon treatment with CP-610431 in experiments conducted between 0.5 and 10 min of duration in which, at concentrations of 50 and 200 nM, maximal inhibition of enzymatic activity of 44 and 87%, respectively, occurred within 30 s of compound addition and was maintained throughout the remainder of the 10-min incubation, consistent with a rapid establishment of an equilibrium between *E* and the various *E*I complex formations. Together, these observations suggest that CP-610431 interacts with the ACC active center at the overlapping acetyl-CoA, citrate, and fatty acyl-CoA binding sites of the second partial reaction, with little interaction with the ATP binding site of the first partial reaction.

Inhibition of Fatty Acid Synthesis, TG Synthesis, and TG Secretion in HepG2 Cells and in Rat Primary Hepatocytes by CP-610431—To assess the ability of CP-497485 to inhibit the cholesterologenic, fatty acid synthetic, TG synthetic, and very low density lipoprotein secretory pathways in cultured cells that express predominately the ACC1 isoform and also to assess its potential to inhibit the human enzyme, CP-497485 was evaluated for its ability to inhibit cholesterol and fatty acid synthesis from [^{14}C]acetate, inhibit TG synthesis from [^{3}H]-glycerol, and inhibit TG and apoB secretion in HepG2 cells. In these studies, CP-497485 inhibited HepG2 cell fatty acid synthesis, TG synthesis, TG secretion, and apoB secretion with respective EC$_{50}$ values of 1.5, 3.0, 3.5, and 9.1 μM, under conditions in which cholesterol synthesis, apoCIII secretion, and cell viability were not altered.

Similar to its improved *in vitro* potency, the active enantiomer, CP-610431, was also considerably more potent than CP-497485 in inhibiting HepG2 cell fatty acid and TG synthesis and in inhibiting TG and apoB secretion. In these studies, CP-610431 dose-dependently inhibited HepG2 cell fatty acid synthesis with an IC$_{50}$ of 1.6 μM, TG synthesis with an IC$_{50}$ of 1.8 μM, TG secretion with an IC$_{50}$ of 3.0 μM, and apoB secretion with an IC$_{50}$ of 5.7 μM (Fig. 3). Similar to its vastly reduced *in vitro* activity, the inactive enantiomer, CP-610432, also did not inhibit HepG2 cell fatty acid synthesis at concentrations up to 100 μM, and showed only modest inhibition of TG synthesis, TG secretion, and apoB secretion, at concentrations of 30 μM.

CP-610431 also inhibited fatty acid synthesis, TG synthesis, and TG secretion in mouse primary hepatocytes with EC$_{50}$ values similar to those noted in HepG2 cells without altering cholesterol synthesis at concentrations of up to 30 μM. In these studies, CP-610431 inhibited mouse primary hepatocyte fatty acid and TG synthesis with IC$_{50}$ values of 0.11 and 1.2 μM and inhibited TG secretion with an IC$_{50}$ of 10 μM.

Inhibition of Mouse Hepatic and Adipose Fatty Acid Synthesis by CP-610431—CP-610431 also inhibited hepatic fatty acid synthesis in fasting CD1 mice by $64 \pm 12\%$ (S.D.; $n = 6$), and $77 \pm 4\%$ (S.D.; $n = 6$), respectively, 1 h after intraperitoneal
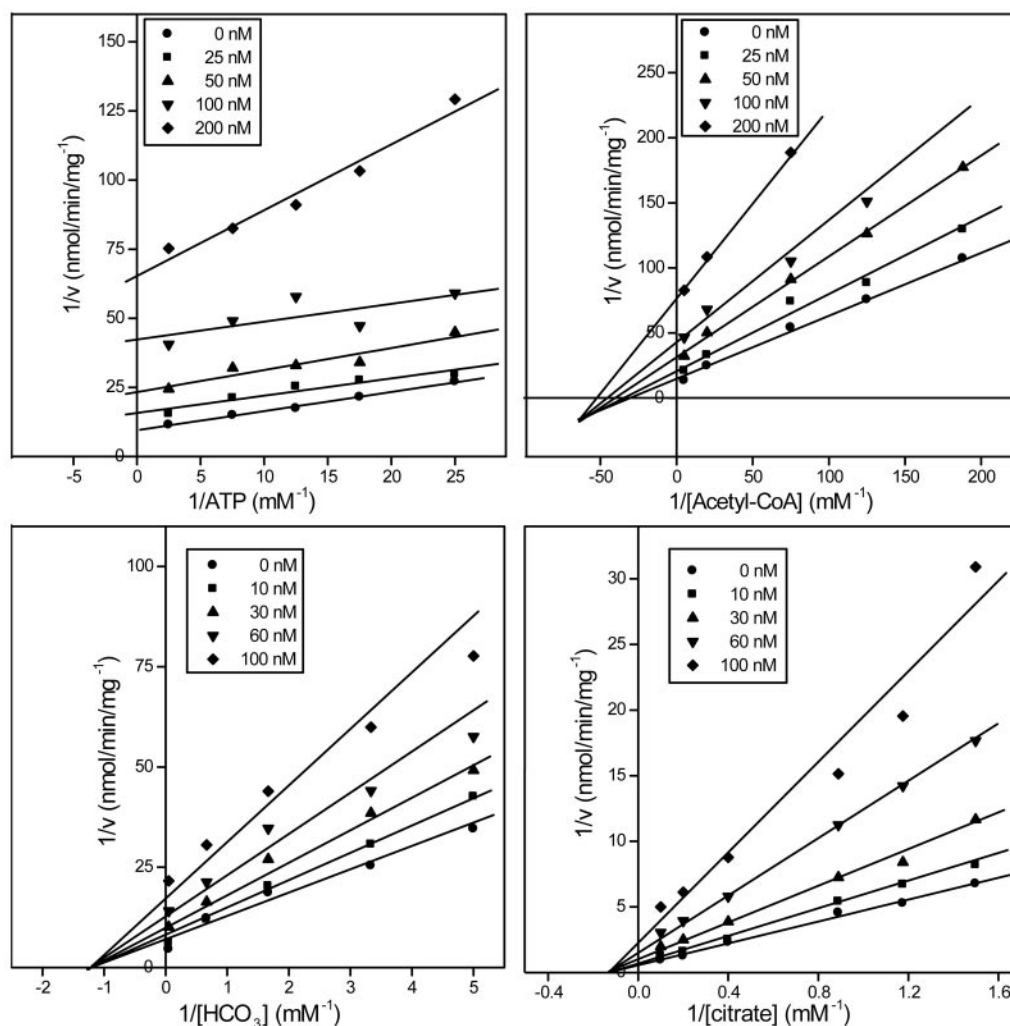
FIG. 2. **Kinetics of ACC1 inhibition by CP-610431.** Aliquots of rat liver ammonium sulfate fraction containing 5.0 μg of protein were incubated with concentrations of ATP between 40 and 400 μM (*upper left panel*), acetyl-CoA between 5 and 200 μM (*upper right panel*), NaH[^{14}C]O$_3$ between 0.2 and 10 mM (*lower left panel*) or citrate between 0.67 mM and 10 mM (*lower right panel*), the remaining ACC substrates and cofactors, and the indicated concentrations of CP-610431 for 10 min at 37 °C as outlined under "Experimental Procedures." After incubation, unreacted NaH[^{14}C]O$_3$ was removed by acidification, the reaction mixture was dried, and the dried residue was resuspended in Redisafe liquid scintillation fluid and assessed for radioactivity as outlined under "Experimental Procedures." Shown is the reciprocal ACC activity (average of duplicate determinations), expressed as nmol/min/mg^{-1}, as a function of reciprocal variable substrate concentration.

administration at doses of 30 and 100 mg/kg. Similar inhibition of hepatic fatty acid synthesis was noted 1 h after intraperitoneal administration of CP-610431 to non-fasting animals (18, 51, and 75% inhibition at 10, 30, and 100 mg/kg), suggesting an ED$_{50}$ of 30 mg/kg. The hydrochloride salt of CP-610431 also showed acute (1 h) oral efficacy, inhibiting hepatic fatty acid synthesis with an ED$_{50}$ of 22 mg/kg. Consistent with the findings above, the inactive enantiomer, CP-610432, was virtually inactive in this model at concentrations of up to 100 mg/kg.

CP-610431 also inhibited hepatic fatty acid synthesis in ob/ob mice within 1 h after dose with an ED$_{50}$ of 3.9 mg/kg. Rates of hepatic fatty acid synthesis in ob/ob mice were ~10 times those of CD1 mice (*e.g.* 352 ± 113 (S.D.; $n = 6$) *versus* 39.7 ± 8.2 (S.D.; $n = 6$) dpm/mg/h), consistent with reports that leptin is a negative regulator of fatty acid synthesis (49, 50). In these studies, CP-610431 also inhibited visceral and subcutaneous adipose tissue fatty acid synthesis with an ED$_{50}$ of ~10 mg/kg, suggesting peripheral exposure suitable for exhibiting efficacy in other nonhepatic tissues. Indeed, at a dose of 10 mg/kg, for example, CP-610431 inhibited hepatic fatty acid synthesis by 64%, visceral adipose fatty acid synthesis by 46%, and subcutaneous adipose tissue fatty acid synthesis by 56%.

Metabolic Instability of CP-610431—Although CP-610431

demonstrated acute *in vivo* fatty acid synthesis inhibition efficacy in short term (1-h) studies, the duration of efficacy of CP-610431 administered intraperitoneally to CD1 mice at a dose of 100 mg/kg was limited to the first 2 h of exposure with no inhibitory activity noted four hours after administration. Evaluation of the hepatic microsomal metabolism of CP-610431 demonstrated average half-lives of 8.5, 7.5, and 7.2 min, respectively, in human liver, rat liver, and CD1 mouse liver microsomes, indicating a P450-mediated metabolic liability of the compound. Half-lives of the inactive enantiomer, CP-610432, in the presence of human and rat liver microsomes averaged 6.6 and 12.4 min, respectively, indicating the absence of enantiomer-specific microsomal metabolism.

In the presence of 1-aminobenzotriazole (ABT; a nonspecific microsomal CYP inhibitor that blocks CYP-mediated microsomal metabolism), given intraperitoneally to CD1 mice at 50 mg/kg, 30 min prior to compound addition, CP-610431 showed an ~10-fold increase in inhibitory activity, inhibiting fatty acid synthesis by 66 and 94% following intraperitoneal administration of doses of 3 and 10 mg/kg, respectively. In these studies, CP-610431 exhibited both an ED$_{50}$ of 3.1 mg/kg, as compared with 24 mg/kg in the absence of ABT treatment, and a marked increase in duration of action such that maximal inhibition of
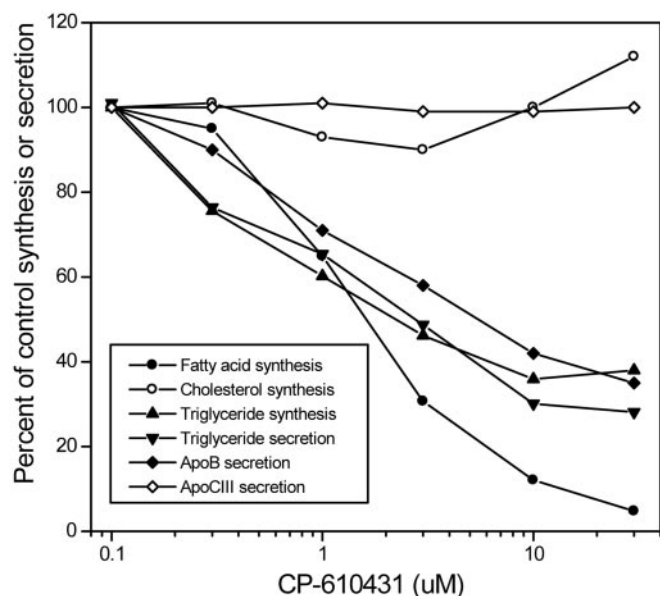
FIG. 3. **Inhibition of HepG2 cell fatty acid synthesis, TG synthesis, TG secretion, and apoB secretion by CP-610431.** For measurement of lipid synthesis and secretion, HepG2 cells seeded and maintained in culture as described under "Experimental Procedures" were incubated for 6 h at 37 °C in supplemented DMEM containing 1% Me_2SO ± CP-610431. For assessment of cholesterol and fatty acid synthesis, cells also received 4 μCi of [2-^{14}C]acetate. After incubation, newly synthesized cholesterol and fatty acids were separated and quantitated as described under "Experimental Procedures." For assessment of TG synthesis and secretion, cells also received 50 μCi of [^{3}H]glycerol. After incubation, the media was removed and the cells were washed three times with PBS, and the secreted (media) and cellular TGs were quantitated as described under "Experimental Procedures." For measurement of apolipoprotein secretion, HepG2 cells seeded and maintained in culture as described under "Experimental Procedures" were incubated for 24 h at 37 °C in supplemented DMEM ± CP-610431. After incubation, the medium was removed and assessed for apoB and apoCIII concentrations by apoprotein-specific enzyme-linked immunosorbent assays as outlined under "Experimental Procedures." Data for lipid synthesis and for lipid and lipoprotein secretion are the mean of triplicate determinations and are expressed as a percentage of control synthesis or secretion as a function of CP-610431 concentration. Control rates of incorporation for the 6-h incubations are as follows: cholesterol synthesis, 87.0×10^3 dpm; TG synthesis, 928×10^3 dpm; TG synthesis 162×10^3 dpm; TG secretion, 27.2×10^3 dpm.

97% occurred 4 h after treatment, with 90 and 47% inhibition noted 8 and 16 h, respectively, after treatment, consistent with CYP-mediated metabolism to a less potent compound. Indeed, biotransformation studies to be published elsewhere[3] identified the main route of metabolism of CP-610431 to be rapid cleavage of an *N*-ethyl group followed by slower loss of the second *N*-ethyl group. Both metabolites were found to be significantly less potent than the parent (IC_{50} = 510 and 1770 nM, respectively), confirming metabolic conversion of CP-610431 to a less active metabolite. Furthermore, the unsubstituted amide and also the free acid (IC_{50} = 10 μM) appeared relatively stable (metabolic half-lives in human liver microsomes of 31 and >45 min, respectively), identifying the diethylamide moiety of CP-610431 as the primary site of metabolism and suggesting minimal microsomal metabolism of other portions of the molecule.

Identification of CP-610431 Analogs with Improved Metabolic Stability—A variety of analogs with presumably improved metabolic stability were prepared and evaluated for intrinsic activity. The activity, microsomal stability, and structure-activity relationships for this series of analogs will be reported

elsewhere.[4] Three of these, however, CP-640188 (diisopropylamide moiety; IC_{50} = 10.5 nM), CP-640189 (di-[2,2,2-trifluoroethyl]amide moiety; IC_{50} = 29 nM), and CP-640186 (morpholinamide moiety; IC_{50} = 70.3 ± 26.1 (S.D.) ± 4.4 (S.E.); n = 35) nM), were subsequently evaluated for their ability to inhibit murine hepatic fatty acid synthesis in the presence and absence of ABT. Both CP-640188 and CP-640189 exhibited a reduced requirement for ABT for maximal efficacy, suggesting improved metabolic stability. For example, when CD1 mice were treated for 1 h at a dose of 3 mg/kg prior to measurement of fatty acid synthesis, CP-610431 reduced fatty acid synthesis by 33% in the absence of ABT and 65% in its presence, whereas, CP-640188 lowered fatty acid synthesis by 53 and 54% and CP-640189 lowered fatty acid synthesis by 59 and 62% in the absence and presence of ABT. Indeed, when evaluated for their rates of hepatic microsomal metabolism, CP-640188 and CP-640189 demonstrated increased average half-lives in the presence of human liver, rat liver, and CD1 mouse liver microsomes of 9.3, 18.9, and 10.6 min, and 9.0, 41.2, and 11.7 min, respectively. Continued improvements in metabolic stability led to identification of CP-640186, which exhibited further improved metabolic half-lives in human liver, rat liver, and mouse liver microsomes of 13.8, >45, and 21.8 min, respectively. Consistent with this improved metabolic stability, CP-640186 demonstrated significant *in vivo* efficacy improvements in mice in the absence of ABT, retaining activity for up to 8 h after administration (see below), and was subsequently selected for additional *in vivo* evaluation.

In Vitro and in Vivo Efficacy of CP-640186—Table II summarizes the *in vitro*, in culture, and acute *in vivo* fatty acid synthesis inhibitory properties of CP-640186. CP-640186 inhibits both ACC1 and ACC2 with a potency of ~55 nM, similar to that observed for CP-610431. However, as a consequence of its improved metabolic stability in hepatic microsomes, CP-640186 exhibited an ~3-fold greater efficacy in inhibiting fatty acid synthesis in HepG2 cells (0.62 *versus* 1.6 μM), and a 2- and 3-fold greater efficacy in inhibiting fatty acid synthesis in CD1 mice (11 *versus* 22 mg/kg) and ob/ob mice (4 *versus* 12 mg/kg) when administered orally in the absence of ABT.

In ob/ob mice, CP-640186 demonstrated acute efficacy for up to 8 h after oral administration, exhibiting ED_{50} values of 4.6, 9.7, and 21 mg/kg, at 1, 4, and 8 h, respectively, after treatment. Threshold efficacy of CP-640186 coincided with plasma drug concentrations of ~150 ng/ml, whereas half-maximal efficacy coincided with plasma drug concentrations of ~350 ng/ml. Peak plasma levels of ~2 μg/ml (10 mg/kg oral dose) coincided with peak efficacy and occurred within 1 h after oral administration, at a time when the liver to plasma drug ratio was ~5. Similarly, in the Sprague-Dawley rat, threshold efficacy occurred at plasma drug concentrations of ~120 ng/ml and half-maximal efficacy occurred at plasma drug concentrations of ~300 ng/ml. Likewise, peak plasma levels also occurred in the rat within 1 h of oral administration, at which time the liver to plasma drug ratio was between 4 and 6. Skeletal muscle concentrations, determined 2 h after oral administration at doses between 10 mg/kg (ED_{50} dose) and 100 mg/kg increased linearly with increasing dose, averaged 154 ng/g of tissue (10 mg/kg) to 1330 ng/g of tissue (100 mg/kg), and mirrored plasma drug concentrations, which averaged 145–1145 ng/ml, respectively.

Pharmacokinetic evaluation of CP-640186 in male Sprague-Dawley rats (intravenous dose, 5 mg/kg; oral dose, 10 mg/kg) yielded a plasma half-life of 1.5 h, a bioavailability of 39%, a Cl_p

[3] V. F. Soliman, D. A. Perry, M. R. Makowski, C. J. Coletta, S. F. Petras, and H. J. Harwood, manuscript in preparation.

[4] D. A. Perry, M. R. Makowski, C. J. Coletta, V. F. Soliman, S. F. Petras, and H. J. Harwood, manuscript in preparation.

TABLE II
Comparison of efficacy and metabolism of CP-610431 and CP-640186

Inhibition of rat liver and rat skeletal muscle ACC activity, inhibition of HepG2 cell fatty acid synthesis and TG synthesis, and acute inhibition of rat, mouse, and ob/ob mouse fatty acid synthesis by CP-610431 and by CP-640186 were determined as described under "Experimental Procedures" and are expressed as the concentration of inhibitor required to prevent by 50% the incorporation of $NaH[^{14}C]O_3$ into malonyl-CoA, the incorporation of $[^{14}C]$acetate into fatty acids, the incorporation of $[^3H]$glycerol into TGs, and the incorporation of $[^{14}C]$acetate into fatty acids, respectively. The half-lives of CP-610431 and CP-640186 in the presence of human, rat, and mouse hepatic microsomes are expressed in terms of time required to produce a 50% reduction in parent concentration.

Parameter	Inhibition by CP-610431	Inhibition by CP-640186
In vitro (IC_{50})		
Rat liver ACC1 inhibition	36 nM	53 nM
Rat skeletal muscle ACC2 inhibition	55 nM	61 nM
In culture (EC_{50})		
HepG2 cell fatty acid synthesis inhibition	1.6 μM	0.62 μM
HepG2 cell TG synthesis inhibition	3.0 μM	1.8 μM
Acute *in vivo* (ED_{50})		
Sprague-Dawley rat fatty acid synthesis inhibition		13 mg/kg
CD1 mouse fatty acid synthesis inhibition	22 mg/kg	11 mg/kg
ob/ob mouse fatty acid synthesis inhibition	12 mg/kg	4 mg/kg
Microsomal metabolism (half-life)		
Human liver microsomes	8.5 min	13.8 min
Rat liver microsomes	7.5 min	>45 min
CD1 mouse liver microsomes	7.2 min	21.8 min

of 65 ml/min/kg, a V_{dss} of 5 liters/kg, an oral T_{max} of 1.0 h, an oral C_{max} of 345 ng/ml, and an oral $AUC_{0-\infty}$ of 960 ng·h/ml. At the same dose level, pharmacokinetic evaluation of CP-640186 in ob/ob mice yielded a plasma half-life of 1.1 h, a bioavailability of 50%, a Cl_p of 54 ml/min/kg, an oral T_{max} of 0.25 h, an oral C_{max} of 2177 ng/ml, and an oral $AUC_{0-\infty}$ of 3068 ng·h/ml. These data indicate that drug exposure is significantly lower in the rat than the ob/ob mouse at equal doses under these conditions, and this may in part explain the greater fatty acid reducing efficacy of CP-640186 in the ob/ob mouse relative to the rat (Table II). Whether this improved exposure is the result of an accumulation of the compound in the substantially larger adipose pool in the ob/ob mouse, which further limits its availability for metabolic clearance, remains to be demonstrated experimentally.

Tissue Malonyl-CoA Lowering by CP-640186—As a consequence of inhibition of ACC1 and ACC2 activity by CP-640186, reductions in fatty acid synthesis in lipogenic tissues such as the liver and adipose tissue, and increases in mitochondrial fatty acid oxidation in oxidative tissues such as the liver, skeletal muscle, and cardiac muscle should be preceded by reductions in tissue malonyl-CoA concentrations. To assess changes in malonyl-CoA concentration in these tissues in response to CP-640186 treatment, the method for assessing tissue malonyl-CoA concentration developed by McGarry *et al.* (42) was adapted to an up to 30 rat/experiment scale (6 groups of 5 animals each), with simultaneous harvesting of soleus muscle, gastrocnemius muscle, quadriceps muscle, adipose tissue, liver, and heart, in the order specified to minimize blood-flow interruption, as outlined under "Experimental Procedures." Tissue malonyl-CoA levels, determined using this modification to McGarry's procedure, expressed as mean ± S.E. ($n = 10$) were as follows: soleus muscle, 1.64 ± 0.13 nmol/g; gastrocnemius muscle, 1.81 ± 0.23 nmol/g; quadriceps muscle, 1.15 ± 0.18 nmol/g; adipose tissue, 0.51 nmol/g; liver, 6.7 ± 0.34 nmol/g; and heart, 1.94 ± 0.15 nmol/g, and compared closely with values reported in the literature (51–53).

The dynamics of the measurement were validated by assessing the ability to modulate tissue malonyl-CoA levels in response to physiological perturbations known to raise and lower tissue malonyl-CoA concentrations in liver and skeletal muscle tissues (16, 54, 55). For example, fasting overnight reduced liver, heart, soleus muscle, and quadriceps muscle malonyl-CoA concentrations by ~60% (Table III), with no further reduction noted when animals were starved for 48 h (not shown), and refeeding either chow (Table III) or a semi-purified high carbohydrate diet (not shown) for 24 h after an overnight fast returned tissue malonyl-CoA concentrations to initial levels.

Single-dose oral treatment with 100 mg/kg CP-640186 also reduced tissue malonyl-CoA concentrations in chow-fed animals such that liver levels were reduced by 58% ($p = 0.009$), heart levels were reduced by 63% ($p = 0.0001$), soleus muscle levels were reduced by 59% ($p = 0.007$), and quadriceps muscle levels were reduced by 80% ($p = 0.002$) within 1 h of administration (Table III). The reduction in malonyl-CoA concentration induced by CP-640186 in all tissues evaluated was dose-dependent with ED_{50} values of 6 mg/kg (soleus muscle), 8 mg/kg (cardiac muscle), 15 mg/kg (quadriceps muscle), and 55 mg/kg (liver) noted 1 h after administration (Fig. 4). Tissue malonyl-CoA levels were also reduced somewhat in fasted animals, but the degree of lowering observed in this already depleted state were considerably diminished in magnitude (Table III).

Stimulation of Fatty Acid Oxidation in C2C12 Rat Skeletal Muscle by CP-640186—The reduction in malonyl-CoA levels that occurs in lipogenic tissues after inhibition of ACC1 by CP-640186 leads to a reduction in fatty acid synthesis both in cultured hepatic cells and in lipogenic tissues of experimental animals (see above). The reduction in malonyl-CoA concentration that occurs in oxidative tissues after inhibition of ACC2 by CP-640186 theoretically should lead to a derepression of mitochondrial CPT-1 activity (malonyl-CoA allosterically inhibits CPT-1 (Refs. 18 and 19)) and an increase in fatty acid utilization in these tissues. In this regard, the acute effects of CP-640186 on skeletal muscle fatty acid metabolism ($[^{14}C]$palmitate oxidation) were assessed in cultured mouse muscle (C2C12) cells and in isolated rat epitrochlearis muscle strips. In both C2C12 cells and muscle strips, CP-640186 increased fatty acid metabolism in a concentration-dependent manner. In C2C12 cells, CP-640186 stimulated $[^{14}C]$palmitate acid oxidation with an EC_{50} of 57 nM and a maximal stimulation of 280% (Fig. 5, *upper panel*). Likewise, in isolated rat epitrochlearis muscle, CP-640186 stimulated $[^{14}C]$palmitate acid oxidation with an EC_{50} of 1.3 μM and a maximal stimulation of 240% (Fig. 5, *lower panel*). The higher EC_{50} value noted in the epitrochlearis muscle presumably reflects tissue penetration differences between the intact muscle bundle and isolated cells. For comparison, in the same experiments, 2.0 mM 5-amino-4-imidazolecarboxamide, *Z*-riboside, which activates AMP-activated protein kinase, leading to phosphorylation and inactivation of ACC (53), stimulated $[^{14}C]$palmitate acid oxidation in C2C12 cells and in isolated rat epitrochlearis muscle by 200 and 210%, respectively.

Stimulation of Rat Fatty Acid Oxidation by CP-640186—CP-640186 also increased whole body fatty acid oxidation acutely in chow-fed and in fasted/high carbohydrate diet-refed rats, shifting energy metabolism away from carbohydrate utilization and toward increased fat utilization. This was demonstrated by assessing the ability of the compound to reduce the RQ, which is a ratio of CO_2 production to O_2 consumption, in resting fed rats (43). Because fatty acids are in a more reduced state than carbohydrates, there is greater amount of oxygen consumed for each CO_2 produced and therefore a lower RQ. If an animal is

TABLE III
Modulation of tissue malonyl-CoA levels by feeding, fasting, and treatment with CP-640186

Twenty-five, Sprague-Dawley rats given food and water *ad libitum* were separated into five groups of 5 animals each. Two groups were maintained on chow and treated orally at a volume of 0.5 ml/200 g of body weight with either an aqueous 0.5% methyl cellulose solution (control vehicle) or a 0.5% methyl cellulose solution containing a 100 mg/kg dose of CP-640186; two groups were fasted for 24 h and then treated as described above, and one group was fasted for 24 h and then refed chow for 48 h. One hour after compound administration, rats were anesthetized with pentobarbital and tissue samples were removed, immediately freeze-clamped, placed in a cryotube, and immersed in liquid N_2 in the order soleus muscle, quadriceps muscle, liver, and heart to minimize blood-flow interruption. Frozen tissues were first pulverized under liquid nitrogen, and then aliquots of the powdered tissues were extracted with 10% HCO_4 and neutralized to pH 6.0 with 5 M KOH. The resultant extracts were then assessed for malonyl-CoA content as outlined under "Experimental Procedures." Data are means ± S.E. ($n = 5$).

Tissue	Tissue malonyl-CoA concentration (nmol/g)				
	Chow-fed	Chow-fed plus CP-640186[a]	Fasted	Fasted plus CP-640186[b]	Fasted, refed
Liver	3.34 ± 0.44	1.40 ± 0.37	2.23 ± 0.22	1.61 ± 0.26	7.39 ± 1.1
Heart	1.91 ± 0.15	0.70 ± 0.04	0.55 ± 0.04	0.23 ± 0.06	1.62 ± 0.20
Soleus	3.01 ± 0.37	1.24 ± 0.32	1.11 ± 0.29	0.69 ± 0.22	3.05 ± 0.56
Quadriceps	1.10 ± 0.15	0.22 ± 0.09	0.40 ± 0.07	0.26 ± 0.06	0.90 ± 0.12

[a] Relative to chow-fed control group: liver, −58% ($p = 0.009$); heart, −63% ($p = 0.0001$); soleus, −59% ($p = 0.007$), quadriceps, −80% ($p = 0.002$).
[b] Relative to fasted control group: liver, −28% (NS); heart, −58% ($p = 0.003$); soleus, −38% (NS); quadriceps, −35% (NS).

utilizing only carbohydrate, RQ = 1.0, whereas if an animal is utilizing only fatty acids, RQ = 0.7.

In the resting state, chow-fed rats exhibited an RQ of ~0.85, indicating a ratio of carbohydrate oxidation to fatty acid oxidation of ~1:1. However, resting rats that had been fasted and then re-fed a high carbohydrate diet (AIN76A) for 2 days prior to experimentation exhibited an RQ of 0.95- 1.05, indicating an almost exclusive utilization of carbohydrate as an energy source. Acute oral treatment of these animals with 100 mg/kg either CP-640186 or CP-640188 resulted in time-dependent reductions in RQ of up to 64 and 89% respectively (Fig. 6, *upper panel*), indicative of a complete shift from carbohydrate utilization to fatty acid utilization as a source of energy at this high exposure level. CP-640186 demonstrated an RQ reduction profile identical to that of a reference standard β3-agonist, CL-316243 (Fig. 6, *upper panel*), reaching maximal RQ reduction after 40 min, consistent with its T_{max} for plasma drug concentration of 45 min, and maintaining that reduced RQ for the duration of the 3-h experiment, again with a time-course of efficacy consistent with the plasma concentration-time profile of the compound. CP-640188, demonstrated a somewhat more rapid approach to maximal RQ reduction, consistent with its shorter T_{max} and demonstrated a modest return toward baseline levels in the later half of the experiment (Fig. 6, *upper panel*), consistent with its shorter half-life in rat liver microsomes (see above).

In contrast to the increase in O_2 consumption noted for the reference standard β3-agonist, neither CP-640186 nor CP-640188 increased total O_2 consumption in these acute experiments (Fig. 6, *lower panel*), consistent with a shift in substrate utilization from carbohydrate oxidation to fatty acid oxidation, without inducing a net increase in oxidative metabolism. Evaluation of CP-640186-mediated RQ reduction at lower doses revealed that RQ reduction was dose-dependent with an ED_{50} value of ~30 mg/kg.

DISCUSSION

In this report we describe potent, isozyme-nonselective inhibitors of mammalian ACC that interact with the enzyme at the site of the allosterically regulated enzymatic carboxyl transfer reaction to equally inhibit the rat, mouse, and cynomolgus macaque ACC1 and ACC2 isozymes with IC_{50} values of ~50 nM. As a consequence of this isozyme-nonselective inhibition, these inhibitors reduce fatty acid synthesis, TG synthesis, and apoB-containing lipoprotein secretion in cultured hepatic cells, and also increase fatty acid oxidation in cultured skeletal muscle cells and tissue slices. Similarly, in experimental animals these inhibitors reduce malonyl-CoA concentration in

both lipogenic (liver and adipose) and oxidative (liver and muscle) tissues, reduce liver and adipose tissue fatty acid synthesis, and increase whole body fatty acid oxidation.

The reaction catalyzed by ACC proceeds via a two-step process, a biotin carboxylase reaction that requires ATP and a carboxyl transferase reaction in which the CO_2 fixed in the first half-reaction is transferred to an acetyl-CoA molecule to form malonyl-CoA (38, 45, 46). ACC inhibitors from this active series interact within the enzyme active center at the site of the carboxyl-transfer reaction, with little interaction with the ATP binding site of the biotin carboxylase reaction. The high degree of specificity of these inhibitors for ACC inhibition relative to inhibition of other mammalian enzymes that catalyze carboxyl transfer reactions, such as pyruvate carboxylase and propionyl-CoA carboxylase, whose carboxyl transfer reaction substrate binding sites are somewhat distinct from that of ACC, is also consistent with their interaction within this region of the ACC active center. Furthermore, that these inhibitors show a high degree of specificity for mammalian ACC relative to fungal ACC, but do show some interaction with the fungal enzyme, is consistent with the low degree of sequence identity of these enzymes (46% overall, 60% carboxyltransferase domain; Refs. 32 and 56) and suggests that these regions of their active centers may be spatially related but are distinct.

As a consequence of their ability to equally inhibit the activity of both ACC1 and ACC2, these isozyme-nonselective ACC inhibitors reduce malonyl-CoA concentration in both lipogenic (liver and adipose) and oxidative (liver and muscle) tissues, reduce liver and adipose tissue fatty acid synthesis, and increase whole body fatty acid oxidation in experimental animals. The studies outlined in this report therefore confirm the hypothesis that reduction in malonyl-CoA production following ACC inhibition leads to a reduction in fatty acid synthesis in lipogenic tissues that express ACC1 and to derepression of CPT-1 activity and consequent increases in fatty acid oxidation in oxidative tissues that express ACC2. In the liver, which is at once both a lipogenic and an oxidative tissue, an isozyme-nonselective ACC inhibitor not only reduces fatty acid synthesis but also increases oxidation of preexisting and incoming fatty acids, leading to reductions in TG formation and in repackaging of TGs into TG-rich apoB-containing lipoproteins, as described above in cultured liver cells.

The NCEP has recently established criteria for identifying persons with the metabolic syndrome (4, 5) and has made recommendations regarding therapeutic intervention. For example, the NCEP established the following five criteria for defining the metabolic syndrome: 1) abdominal obesity, waist circumference >102 cm (men) and >88 cm (women); 2) hyper-
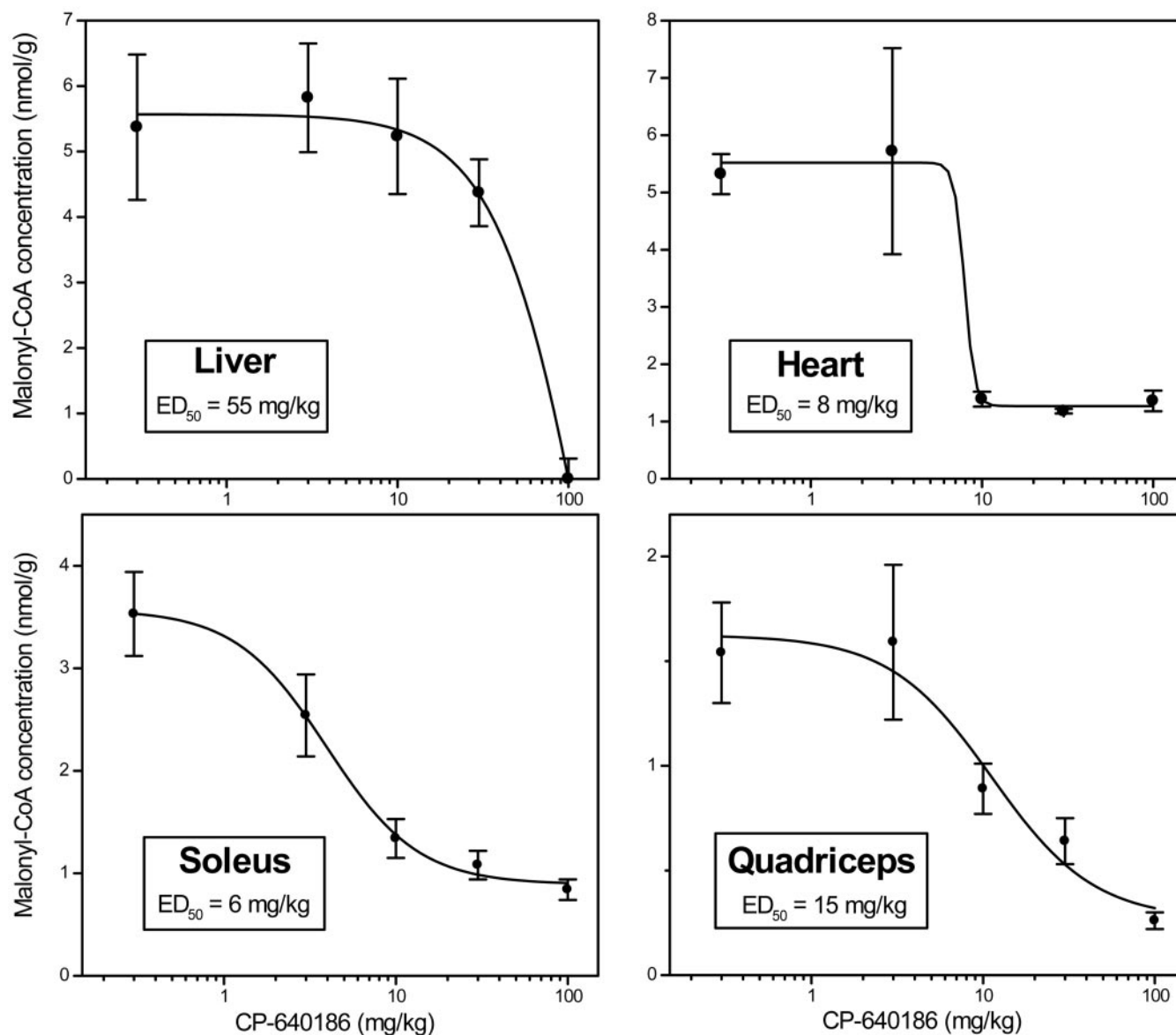
FIG. 4. **Tissue malonyl-CoA lowering by CP-640186.** Thirty Sprague-Dawley rats given food and water *ad libitum* were treated orally at a volume of 0.5 ml/200 of g body weight with either an aqueous 0.5% methyl cellulose solution or a 0.5% methyl cellulose solution containing the indicated doses of CP-640186. One hour after compound administration, rats were anesthetized with pentobarbital and tissue samples were removed, immediately freeze-clamped, placed in a cryotube, and immersed in liquid N_2 in order soleus muscle, quadriceps muscle, liver, and heart to minimize blood-flow interruption. Frozen tissues were first pulverized under liquid N_2 then aliquots of the powdered tissues were extracted with 10% $HClO_4$ and neutralized to pH 6.0 with 5 M KOH. The resultant extracts were then assessed for malonyl-CoA content as outlined under "Experimental Procedures." Shown is the tissue malonyl-CoA concentration, expressed in nanomoles/g of tissue as a function of dose of CP-640186.

triglyceridemia, >150 mg/dl; 3) low HDL cholesterol, < 40 mg/dl (men), < 50 mg/dl (women); 4) hypertension, >135/85 mm Hg; and 5) fasting glucose >110 mg/dl (4, 5). The NCEP has further designated anyone presenting with any three of the five criteria as possessing the metabolic syndrome and therefore being at increased cardiovascular risk (4, 5).

By increasing fatty acid oxidation in the liver and skeletal muscles, by reducing *de novo* fatty acid synthesis in the liver and adipose tissue, and by reducing TG-rich apoB-containing lipoprotein secretion from the liver, an isozyme-nonselective ACC inhibitor has the potential to favorably affect most if not all of the cardiovascular risk factors associated with the metabolic syndrome. Indeed, as outlined in a subsequent report,[2] the actions of these isozyme-nonselective ACC inhibitors have been shown to lead to reductions in liver, skeletal muscle, and adipose tissue TG levels and subsequently to reductions in whole body fat mass, reductions in body weight, and improve-

ments in insulin sensitivity with chronic treatment of dietarily induced rat models of the metabolic syndrome.

Isozyme-nonselective ACC inhibitors have the advantage of the combined actions of ACC1 inhibition and ACC2 inhibition, and as such would possess the maximal potential for beneficially effecting the metabolic syndrome through this mechanism of action. A recent report describing the phenotype of ACC2 knock-out mice (34) has suggested that an ACC2 isozyme-selective inhibitor would also have beneficial effects on the cardiovascular risk factors associated with the metabolic syndrome. However, although these animals presented with a phenotype demonstrating a reduction in skeletal muscle malonyl-CoA concentrations, an increase in rates of muscle fatty acid oxidation, a reduced hepatic fat content, a reduction in total body fat in the face of a somewhat greater food consumption, and a reduction in plasma glucose and free fatty acid concentration relative to wild-type liter-mates, it was clear that
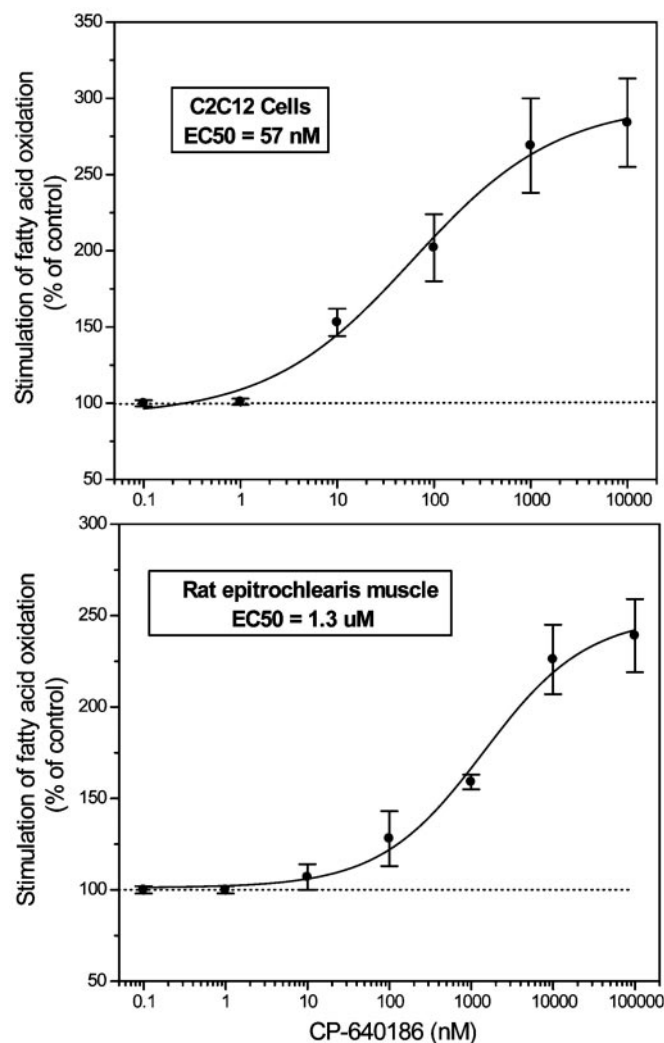
FIG. 5. **Stimulation of fatty acid oxidation in cultured skeletal muscle C2C12 cells and in epitrochlaris muscle slices by CP-640186.** C2C12 cells, seeded and maintained in culture as described under "Experimental Procedures" (*upper panel*) and rat epitrochlearis muscle strips, prepared as described under "Experimental Procedures" (*lower panel*) were incubated for 2 h at 37 °C in a shaking water bath with the indicated concentrations of CP-640186 in the presence of [^{14}C]palmitate (3.4 μCi; 1.0 μCi/μmol). After incubation, the reaction was terminated by addition of 60% perchloric acid, released $^{14}CO_2$ was captured by a 300-μl volume of benzethonium hydroxide, and the captured $^{14}CO_2$ was quantitated as outlined under "Experimental Procedures." Shown is the percentage of control fatty acid oxidation as a function of CP-640186 concentration. Data are means $\pm$ S.E. for $n = 3$ experiments performed in duplicate.

FIG. 6. **Stimulation of rat fatty acid oxidation (respiratory quotient lowering) by CP-640186.** Twenty male Sprague-Dawley rats (350–400 g) given food and water *ad libitum*, were fasted and then refed a high sucrose diet (AIN76A) for 2 days prior to experimentation. An additional eight rats, maintained on standard laboratory chow, were fasted for 24 h prior to study. On the day of study, rats were placed into sealed chambers of a pre-calibrated Oxymax open circuit, indirect calorimeter (one rat per chamber), and base-line CO_2 production, O_2 consumption, RQ, and ambulatory activity were measured every 10 min for 2 h as outlined under "Experimental Procedures." After collecting base-line data, the chambers were opened and rats are given a 1.0-ml oral bolus of either an aqueous 0.5% methylcellulose solution (AIN76A fed ($n = 8$) and fasted ($n = 8$) controls), or an aqueous 0.5% methylcellulose solution containing either 100 mg/kg CP-640186 ($n = 4$), 100 mg/kg CP-640188 ($n = 4$), or 1 mg/kg CL-316243 ($n = 4$), and then returned to the Oxymax chambers. Measurements of CO_2 consumption, O_2 consumption, RQ, and ambulatory activity were made every 10 min for an additional 3 h. Shown are the 10-min incremental oxygen consumption and RQ values for the AIN76A-fed (*closed squares*) and fasted (*open squares*) control animals and for the CP-640186-treated (*closed circles*), CP-640188-treated (*closed triangles*), and CL-316234-treated (*open triangles*) animals as a function of time after compound administration.

the liver and possibly also the adipose tissues were compensating to some degree for the lack of ACC2-mediated control of fatty acid oxidation by increasing ACC1-mediated fatty acid synthesis (34). Whether an ACC2 isozyme-specific inhibitor would be as efficacious in experimental animals as an isozyme-nonspecific ACC inhibitor or would have its efficacy attenuated by compensatory increases in hepatic and adipose tissue fatty acid synthesis remains to be determined experimentally.

Similarly, an ACC1 isozyme-selective inhibitor should favorably affect liver and adipose tissue fatty acid synthesis and also hepatic TG-rich apoB-containing lipoprotein secretion. Indeed, the liver-specific ACC inhibitor TOFA reduced fatty acid synthesis and TG secretion both in cultured hepatic cells (24, 27) and in experimental animals (23, 26, 28), and reduced plasma cholesterol and TGs in experimental animals including Rhesus monkeys (23, 27). However, the theoretical lack of effectiveness
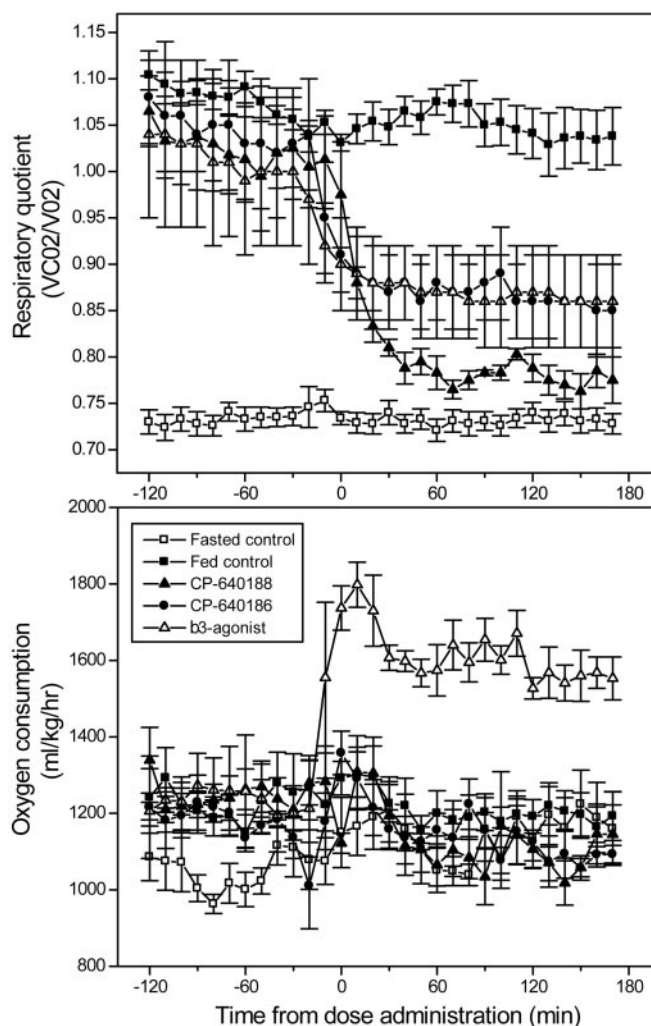
of an ACC1 isozyme-selective inhibitor in directly improving skeletal muscle fatty acid metabolism may limit its ability to favorably affect the etiology of the metabolic syndrome. Whether the effects of an ACC1 isozyme-selective inhibitor would be sufficient to favorably affect the metabolic syndrome also remains to be determined experimentally.

Taken together, the observations outlined in this report provide convincing evidence that isozyme-nonselective inhibition of ACC activity can inhibit ACC2 activity in oxidative tissues, such as the liver and skeletal muscle, and can simultaneously inhibit the activity of ACC1 in lipogenic tissues, such as the

liver and adipose, and prevent any compensatory increases in fatty acid synthesis from attenuating the ACC2 inhibition-mediated increases in fatty acid oxidation, and would therefore have the optimal therapeutic potential for treating the multiple sequelae of the metabolic syndrome.

REFERENCES

1. Reaven, G. M. (1988) *Diabetes* **37,** 1595–1607
2. Howard, B. V. (1995) in *Atherosclerosis X* (Woodford, F. P., Davignon, J., and Sniderman, A, eds) pp. 516–519, Elsevier Science B.V., New York
3. Crepaldi, G. (1995) in *Atherosclerosis X* (Woodford, F. P., Davignon, J., and Sniderman, A, eds) pp. 511–515, Elsevier Science B.V., New York
4. Ford, E. S., Giles, W. H., and Dietz, W. H. (2002) *J. Am. Med. Assoc.* **287,** 356–359
5. National Cholesterol Education Program Expert Panel (2001) *J. Am. Med. Assoc.* **285,** 2486–2497
6. Alberti, K. G. M. M., and Zimmet, P. Z. (1998) *Diabet. Med.* **15,** 539–553
7. Moller, D. E. (2001) *Nature* **414,** 821–827
8. Grundy, S. M. (1999) *Am. J. Cardiol.* **83,** 25F–29F
9. Haffner, S. M., Valdez, R. A., Hazuda, H. P., Mitchell, B. D., Morales, P. A., and Stren, M. P. (1992) *Diabetes* **41,** 715–722
10. Isomaa, B., Almgren, P., Tuomi, T., Forsen, B., Lahti, K., Nissen, M., Taskinen, M. R., and Groop, L. (2001) *Diabetes Care* **24,** 683–689
11. Trevisan, M., Liu, J., Bahsas, F. B., and Menotti, A. (1998) *Am. J. Epidemiol.* **148,** 956–966
12. Bjorntorp, P. (1994) *Curr. Opin. Lipidol.* **5,** 166–174
13. Depres, J. P., and Marette, A. (1994) *Curr. Opin. Lipidol.* **5,** 274–289
14. McGarry, J. D. (1992) *Science* **258,** 766–770
15. Kim, K. H. (1997) *Annu. Rev. Nutr.* **17,** 77–99
16. McGarry, J. D., and Foster, D. W. (1980) *Annu. Rev. Biochem.* **49,** 395–420
17. Munday, M. R., and Hemingway, C. J. (1999) *Adv. Enzyme Reg.* **39,** 205–234
18. McGarry, J. D., Woeltje, K. F., Kuwajima, M., and Foster, D. W. (1989) *Diabetes Metabol. Revs.* **5,** 271–284
19. McGarry, J. D., and Brown, N. F. (1997) *Eur. J. Biochem.* **244,** 1–14
20. Rasmussen, B. B., Holmback, U. C., Volpi, E., Morio-Liondore, B., Paddon-Jones, D., and Wolfe, R. R. (2002) *J. Clin. Invest.* **110,** 1687–1693
21. Chen, S., Ogawa, A., Ohneda, M., Unger, R. H., Foster, D. W., and J. D. McGarry (1994) *Diabetes* **43,** 878–883
22. Brun, T., Roche, E., Assimacopoulos-Jeannet, F., Corkey, B. E., Kim, K. H., and Prentki, M. (1996) *Diabetes* **45,** 190–198
23. Parker, R. A., Kariya, T., Grisar, J. M., and Petrow, V. (1977) *J. Med. Chem.* **20,** 781–791
24. McCune, S. A., and Harris, R. A. (1979) *J. Biol. Chem.* **254,** 10095–10101
25. Triscari, J., and Sullivan, A. C. (1984) *Int. J. Obesity* **8,** Suppl. 1, 227–239
26. Fukuda, N., and Ontko, J. A. (1984) *J. Lipid Res.* **25,** 831–842
27. Arbeeny, C. M., Meyers, D. S., Bergquist, K. E., and Gregg, R. E. (1992) *J. Lipid Res.* **33,** 843–851
28. Kempen, H. J., Imbach, A. P., Giller, T., Neumann, W. J., Hennes, U., and Nakada, N (1996) *J. Lipid Res.* **36,** 1796–1806
29. Bianchi, A., Evans, J. L., Iverson, A. J., Nordlund, A. C., Watts, T. D., and Witters, L. A. (1990) *J. Biol. Chem.* **265,** 1502–1509
30. Iverson, A. J., Bianchi, A., Nordlund, A. C., and Witters, L. A. (1990) *Biochem. J.* **269,** 365–371
31. Widmer, J., Fassihi, K. S., Schlichter, S. C., Wheeler, K. S., Crute, B. E., King, N., Nutile-McMenemy, Noll, W. W., Daniel, S, Ha, J., Kim, K. H., and Witters, L. A. (1996) *Biochem. J.* **316,** 915–922
32. Ha, J., Lee, J. K., Jim, K. S., Witters, L. A., and Kim, K. H. (1996) *Proc. Nat'l. Acad. Sci. U. S. A.* **93,** 11466–11470
33. Abu-Elheiga, L., Almarza-Ortega, D. B., Baldini, A., and Wakil, S. J. (1997) *J. Biol. Chem.* **272,** 10669–10677
34. Abu-Elheiga, L., Matzuk, M. M., Abo-Hashema, K. A. H., and Wakil, S. J. (2001) *Science* **291,** 2613–2616
35. Whittington, M., Esner, M., Pratt, J., Riddell, D., and Ashton, M. J. (1987) *Int. J. Obesity* **11,** 619–629
36. Harwood, H. J., Jr., Barbacci-Tobin, E. G., Petras, S. F., Lindsey, S., and Pellarin L. D. (1997) *Biochem. Pharmacol.* **53,** 839–864
37. Petras, S. F., Lindsey, S., and Harwood, H. J., Jr. (1999) *J. Lipid Res.* **40,** 24–38
38. Thampy, K. G., and Wakil, S. J. (1985) *J. Biol. Chem.* **260,** 6318–6323
39. Haghpassand, M., Wilder, D. E., and Moberly, J. B. (1996) *J. Lipid Res.* **37,** 1468–1480
40. Haghpassand, M., and Moberly. J. B., (1995) *Atherosclerosis* **117,** 199–207
41. Harwood H. J., Jr., Silva, M., Chandler, C. E., Mikolay, L., Pellarin, L. D., Barbacci-Tobin, E., Wint, L. T., and McCarthy, P. A. (1990) *Biochem. Pharmacol.* **40,** 1281–1293
42. McGarry, J. D., Stark, M. J., and Foster, D. W. (1978) *J. Biol. Chem.* **253,** 8291–8293
43. Ferrannini, E. (1988) *Metabolism* **37,** 287–301
44. Tanabe, T., Nakanishi, S., Hashimoto, T., Ogiwara, H., Nikawa, J. I., and Numa, S. (1981) *Methods Enzymol.* **71,** 5–16
45. Hashimoto, T and Numa, S. (1971) *Eur. J. Biochem.* **18,** 319–331
46. Beaty, N. M., and Lane, M. D. (1982) *J. Biol. Chem.* **257,** 924–929
47. Trumble, G. E., Smith, M. A., and Winder, W. W. (1995) *Eur. J. Biochem.* **231,** 192–198
48. Ogiwara, T., Tanabe, T., Nikawa, J. I., and Numa, S. (1978) *Eur. J. Biochem.* **89,** 33–41
49. Minokoshi, Y., Kim, Y. B., Peroni, O. D., Fryer, L. G. D., Muller, C., Carling, D., and Kahn, B. B. (2002) *Nature* **415,** 339–343
50. Bai, Y., Zhang, S., Jim, K. S., Lee, J. K., and Kim, K. H. (1996) *J. Biol. Chem.* **271,** 13939–13942
51. Chien, D., Dean, D., Saha, A. K., Flatt, J. P., and Ruderman, N. B. (2000) *Am. J. Physiol.* **279,** E259–E265
52. Winder, W. W., Arogyasami, J., Elayan, I. M., and Cartmill, D. (1990) *Am. J. Physiol.* **259,** E266–E271
53. Kudo, N., Barr, A. J., Barr, R. L., Desai, S., and Lopaschuk, G. D. (1995) *J. Biol. Chem.* **270,** 17513–17520
54. Buckley, M. G., and Rath, E. A. (1987) *Biochem. J.* **243,** 437–442
55. Saha, A. K., Kurowski, T. G., and Ruderman, N. B. (1995) *Am. J. Physiol.* **269,** E283–E289
56. Al-Feel, W., Chirala, S. S., and Wakil, S. J. (1992) *Proc. Natl. Acad. Sci. U. S. A.* **89,** 4534–4538